



THE  
2  
2006

**LIBRARY  
Michigan State  
University**

This is to certify that the  
thesis entitled

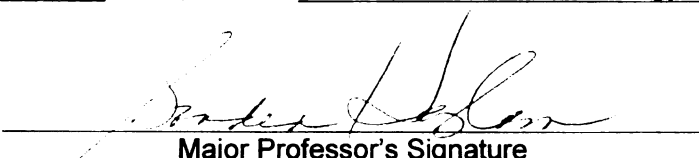
ANALYSIS OF PROGESTIN EFFECTS ON HEPATOCYTE  
GROWTH FACTOR SIGNALING PATHWAYS IN RELATION TO  
PROLIFERATION AND ALVEOLAR MORPHOGENESIS OF  
NORMAL MAMMARY EPITHELIAL CELLS *IN VITRO*

presented by

Kyle Thomas Smith

has been accepted towards fulfillment  
of the requirements for the

M.S. degree in Cell and Molecular Biology

  
Major Professor's Signature

12-05-05

Date

**PLACE IN RETURN BOX** to remove this checkout from your record.  
**TO AVOID FINES** return on or before date due.  
**MAY BE RECALLED** with earlier due date if requested.

DATE DUE	DATE DUE	DATE DUE

ANALYSIS OF PROGESTIN EFFECTS ON HEPATOCYTE GROWTH FACTOR  
SIGNALING PATHWAYS IN RELATION TO PROLIFERATION AND ALVEOLAR  
MORPHOGENESIS OF NORMAL MAMMARY EPITHELIAL CELLS *IN VITRO*

By

Kyle Thomas Smith

A THESIS

Submitted to  
Michigan State University  
in partial fulfillment of the requirements  
for the degree of

MASTER OF SCIENCE

CELL AND MOLECULAR BIOLOGY PROGRAM

2005



## ABSTRACT

### ANALYSIS OF PROGESTIN EFFECTS ON HEPATOCYTE GROWTH FACTOR SIGNALING PATHWAYS IN RELATION TO PROLIFERATION AND ALVEOLAR MORPHOGENESIS OF NORMAL MAMMARY EPITHELIAL CELLS *IN VITRO*

By

Kyle Thomas Smith

Progestins (P) are major mitogens in the adult human breast and can significantly contribute to breast cancer risk. Using an *in vitro*, primary culture system we determined that for P-induced proliferation and morphogenesis to occur in normal mouse mammary cells, the presence of hepatocyte growth factor (HGF) is required. HGF induces proliferation and ductal morphogenesis. Addition of P results in increased proliferation and alveolar-like morphogenesis.

The aim was to determine the cell type specific signaling pathways by which P and HGF interact to promote growth and morphology change of mammary epithelial organoids, containing luminal and myoepithelial cells. This was done by immunostaining of HGF signaling intermediates and using biochemical inhibitors of relevant signaling pathways, PI3K, MEK1/2, and matrix metalloproteinases (MMPs). Results showed that increased expression of cyclin D1 and PR B, and decreased expression of PRA in luminal cells was correlated with increased proliferation and alveolar-like morphology response to HGF+P treatment; no changes in c-Met expression were observed in either cell type under any treatment. Both PI3K and MEK1/2 signaling intermediates were important for the proliferative response of luminal cells and morphologic responses of myoepithelial cell treated with HGF+P. MMPs activity was important for proliferative and morphologic responses of luminal cells only.



## TABLE OF CONTENTS

LIST OF FIGURES.....	v
KEY TO SYMBOLS OR ABBREVIATIONS.....	ix
INTRODUCTION.....	1
Progesterone has Major Mitogenic Activity in the Human Adult Mammary Gland.....	1
The Mouse Model.....	1
Mammary Gland Organization and the Epithelial Subtypes of the Mammary Gland.....	2
Mammary Gland Development in the Mouse.....	4
The Role of Progesterone in Mammary Epithelial Cell Proliferation in the Mouse.....	6
Mechanisms of Progesterone Action.....	7
Knock-out Studies and Progesterone Action.....	10
Stromal Cell Influences on Mammary Gland Development.....	13
Hepatocyte Growth Factor and its Receptor, c-Met.....	13
Models of Hepatocyte Growth Factor-Induced Tubulogenesis.....	15
An <i>In Vitro</i> Model to Study Progesterone-Induced Proliferation.....	17
Signaling Pathways Relevant to Proliferation, Morphogenesis, and Interactions between Hepatocyte Growth Factor and Progesterone.....	20
Matrix Metalloproteinases (MMPs) and Mammary Development.....	22
Hypothesis.....	23
METHODS.....	25
Animals.....	25
Cell Culture.....	25
<i>In Situ</i> Labeling of Mammary Organoids in Collagen Gels.....	26
Immunohistochemistry.....	27
Determination of Proliferation in Primary Organoid Cultures.....	28
<sup>3</sup> H]Thymidine incorporation assay.....	28
BrdU Incorporation and Analysis of Cell Type Specific Proliferation.....	28
Immunohistochemistry Quantitation Methods.....	29
General Criteria for Quantitation.....	29
PR Isoform Quantitation.....	29
c-Met Quantitation.....	29
Cyclin D1 Quantitation.....	30
Inhibitor Studies.....	30
Cell Viability Staining.....	31
RESULTS.....	32
The Roles of Luminal Epithelial and Myoepithelial Cells in Mammary Organoids Morphology.....	32
Cell Type Specific Proliferation <i>In Vitro</i> .....	33

<i>In Vivo</i> Expression of c-Met Protein During Mouse Mammary Gland Development.....	34
<i>In Vitro</i> Expression of c-Met Protein in Response to Culture Treatments.....	35
<i>In Vitro</i> Expression of Cyclin D1 Protein.....	36
<i>In Vitro</i> PR Isoform Protein Expression.....	37
PR A Protein Expression.....	37
PR B Protein Expression.....	38
c-Met Signaling Pathway Inhibitor Studies.....	38
PI3K Pathway.....	39
Effect of PI3K and AKT Inhibitors on Proliferation.....	39
Effect of PI3K and AKT Inhibitors on Cell Type Specific Morphology of Mammary Organoids.....	40
ERK Pathway.....	41
Effect of MEK 1/2 Inhibitor on Proliferation.....	42
Effect of MEK 1/2 Inhibitor on Cell Type Specific Morphology of Mammary Organoids.....	42
Matrix Metalloproteinase Inhibition.....	43
Effect of MMP Inhibitor on Proliferation.....	43
Effect of MMP Inhibitor on Cell Type Specific Morphology of Mammary Organoids.....	43
DISCUSSION.....	61
The Roles of Luminal Epithelial and Myoepithelial Cells in Mammary Organoid Morphology.....	61
Cell Type Specific Proliferation.....	64
c-Met Protein Expression.....	65
<i>In Vivo</i> Studies.....	65
<i>In Vitro</i> Studies.....	66
Cyclin D1.....	68
PR Isoform Protein Expression.....	69
Inhibitor Treatment of Cultures.....	71
PI3K/AKT.....	72
ERK 1/2.....	75
Matrix Metalloproteinases.....	77
Summary.....	80
REFERENCES.....	82

## LIST OF FIGURES

Figure 1. Diagram of <i>in vivo</i> architecture of mouse mammary duct. Figure created by Alexis Drolet.....	5
Figure 2. Development of mouse mammary gland from birth to sexual maturity. Figure created by Alexis Drolet.....	8
Figure 3. Development of the mouse mammary gland during pregnancy. Figure created by Alexis Drolet.....	9
Figure 4. Effect of progestin (R5020) on epithelial cell proliferation in collagen gels. Mammary epithelial cells in collagen gels were cultured alone (BM+Hormones) or with HGF (50ng/ml). For each of these conditions cells also received treatment with basal media only (BM), Estradiol 20nM (E2), R5020 10nM, or E2+R5020 (20nM+10nM). 3H-thymidine incorporation was assayed on day 3. The data are expressed as fold increases over basal media. Each bar = mean $\pm$ S.E.M. of triplicate determination from 3-5 separate experiments. * p = 0.05 that proliferation in HGF+R5020 treated cultures is greater than HGF and HGF+E2-treated cultures within each treatment group. ** p = 0.05 that proliferation in HGF+E2+R5020 is greater than all other treatments within each treatment group. Endocrinology Vol. 143, No. 8 2953-2960.....	22
Figure 5. Phase contrast photomicrographs of epithelial cell organoid morphology in collagen gel cell culture. Mammary epithelial cells were suspended in collagen I gels and cultured for 3 d in BM, E2, PRL (1 $\mu$ g/ml), R5020, HGF, or R5020+HGF. Gross organoid morphology was visualized <i>in situ</i> in collagen gels with the aid of an inverted microscope (magnification, x100) and in histological sections of collagen gels (magnification, x400). Organoids appear solid when treated with BM, E2, and PRL, whereas lumens (L), tubules (T), and alveolar buds (AB) are visible in R5020, HGF, and R5020 plus HGF cultures, respectively. Sections through a tubule and alveolar structure are also shown. Endocrinology Vol. 143, No. 8 2953-2960.....	23
Figure 6. Luminal epithelial and myoepithelial cell morphologies in response to culture treatments. Images are a projection images constructed from a z-series captured on a confocal microscope. Organoids were treated with BM, HGF, R5020, and HGF+R5020. Green images are stained with phalloidin conjugated with Alexa-488 which stained actin, and labeled all cells. Red images are stained for smooth muscle actin (SMA), which is a specific marker of myoepithelial cells. Note the elongated myoepithelial cells in the HGF- and HGF+R5020-treated organoids and the cyst of luminal cells surrounded by myoepithelial cells in the R5020-treated organoid (mag. 200X).....	48

Figure 7. Time course of luminal and myoepithelial cell morphology in HGF-treated organoids. Images are projection images constructed from a z-series captured on a confocal microscope. Red images are stained for smooth muscle actin (SMA), which is a specific marker of myoepithelial cells. Overlay image is the combination of SMA staining and the staining of organoids with phalloidin conjugated with Alexa-488, which stained actin, and labeled all cells. White arrows indicate cellular extensions of luminal cells. Yellow arrows indicate myoepithelial cells in extensions. Note that luminal epithelial cells and not myoepithelial cells were at the leading edge of extensions. (mag. 200x).....49

Figure 8. Cell type specific proliferation at 72hrs. A. Representative staining of HGF and HGF+R5020 treated organoids. Blue staining represents cell nuclei. Green staining represents BrdU positive cells. Red staining cells are positive for the myoepithelial marker, smooth muscle actin (SMA). The merge image is a composite of the three other images. White arrows indicate proliferating myoepithelial cells, which are only present in HGF+R5020 treated organoids. Yellow arrows indicate proliferating luminal cells and blue arrows indicate myoepithelial cells that are not proliferating. (mag. 400x) B. Quantitation of average BrdU positive cells per organoid section. White bars indicate the mean number of luminal epithelial cells proliferating per organoid section  $\pm$  SEM. Black bars indicate the mean number of myoepithelial cells proliferating per organoid section  $\pm$  SEM.....50

Figure 9. Analysis of expression of c-Met during the mammary gland developmental stages of puberty (5wks), sexual maturity (10wks), pregnancy (ducts and alveoli), and lactation (ducts and alveoli). Comparison of c-Met expression in luminal epithelial vs. myoepithelial cells. Each bar = mean  $\pm$  S.E.M.....51

Figure 10. Effect of culture treatments on c-Met protein expression in epithelial organoids cultured in collagen gels. Mammary epithelial cells in collagen gels were cultured alone (BM), in R5020 (10nM), in HGF (50ng/ml), or in HGF (50ng/ml) + R5020 (10nM) (H+R). A. Expression of c-Met within luminal epithelial cells, B. Expression of c-Met within myoepithelial cells. C. Expression of c-Met in luminal epithelial cells vs. myoepithelial cells. Each bar = mean  $\pm$  S.E.M.....52

Figure 11. Cyclin D1 expression in adult cultured organoids A. Representative images showing D1 expression in adult cultured organoids. Green images represent D1 expression, red images represent myoepithelial cells, and blue images represent the nuclei of all cells in the organoid. The merged image is an overlay of the three separate images. (mag. 630x) B. Nuclear localization of Cyclin D1. Percentage of cells expressing cyclin D1 localized in the nucleus under treatments of BM, HGF, R5020 (R), and HGF+R5020 (H+R) Each bar = mean  $\pm$  range (n = 2).....53

Figure 12. PRA expression in cultured organoids. The results presented are averages of three different cultures (cc1-20-04, cc1-26-04, and cc1-18-05). A. PR A expression at 48hrs. Percentage of total cells positive for PR A at time points of 48hrs. B. PR A expression at 72hrs. Percentage of total cells positive for PR A at time points 72hrs. Organoids were treated with BM, HGF (H), R5020 (R), HGF+R5020 (H+R), and estrogen (E). Each bar = mean  $\pm$  SEM. Number in bars indicates the total number of organoids sampled from all cultures. Due to sample size and variability no statistical analysis was performed.....54

Figure 13. PRB expression in cultured organoids. The results presented are the average of two separate cultures (cc1-20-04 and cc1-26-04). A. PR B expression at 48hrs. Percentage of total cells positive for PR A at time points of 48hrs. B. PR B expression at 72hrs. Percentage of total cells positive for PR B at time points 72hrs. Organoids were treated with BM, HGF (H), R5020 (R), HGF+R5020 (H+R), and estrogen (E). Each bar = mean  $\pm$  standard deviation. Number in bars indicates the total number of organoids sampled from all cultures. Due to sample size and variability no statistical analysis was performed.....55

Figure 14. Effects of PI3K and AKT inhibition on HGF- and R5020-dependent proliferation at 72hrs. A. Effect of PI3K inhibition. Fold increase in proliferation measured by 3H-thymidine incorporation was calculated versus BM of control treatments under an inhibitor concentration of 5 $\mu$ M LY294002 . B. Effect of PI3K inhibition. 3H-tdr incorporation as a percentage of corresponding control treatment. C. Effect of AKT inhibition. Fold increase in proliferation measured by 3H-tdr incorporation was calculated versus BM of control treatments under an inhibitor concentration of 200 nM AKT inhibitor IV. D. Effect of AKT inhibition. 3H-thymidine incorporation as a percentage of corresponding control treatment. Each bar = mean  $\pm$  SEM.....56

Figure 15. PI3K inhibitor effects on organoid, luminal, and myoepithelial cell morphologies. Images are a projection images constructed from a z-series captured on a confocal microscope. Organoids were treated as indicated. Green images were stained with phalloidin conjugated with Alexa-488, which stained actin, and labeled all cells. Red images are stained for smooth muscle actin (SMA), which is a specific marker of myoepithelial cells. Note the reduction of SMA expressing cells in LY294002-treated cultures, especially in HGF and HGF+R5020 treatments. White arrows indicate the reduction of SMA labeling (mag. 200x).....57

Figure 16. AKT inhibitor effects on organoid, luminal and myoepithelial cell morphologies. Images are a projection images constructed from a z-series captured on a confocal microscope. Organoids were treated as indicated. Green images were stained with phalloidin conjugated with Alexa-488, which stained actin, and labeled all cells. Red images are stained for smooth muscle actin (SMA), which is a specific marker of myoepithelial cells. Note the absence of SMA expressing cells in AKT inhibitor IV-treated organoids (mag. 200x).....58

Figure 17. Time course of luminal and myoepithelial cell morphology in HGF-treated organoids in the presence of 5 $\mu$ M LY. Images are a projection images constructed from a z-series captured on a confocal microscope. Red images are stained for smooth muscle actin (SMA), which is a specific marker of myoepithelial cells. Green image is the staining of organoids with phalloidin conjugated with Alexa-488, which stained actin, and labeled all cells. Note that SMA expressing cells are present at 24hrs of LY294002 treatment and are lost by 72hrs. Wash-out of PI3K inhibitor at 24hrs resulted in the rescue of SMA expressing cells at 72hrs. (mag. 200x).....59

Figure 18. A. Effect of MEK 1/2 inhibition on proliferation at 72hrs. A. Fold increase in proliferation determined by 3H-tdr incorporation was calculated versus BM of control treatments. A concentration of 10 $\mu$ M U0126 was used. B. Effect of MEK1/2 inhibition. Percentage of 3H-tdr incorporation as a percentage of corresponding control treatment. Each bar = mean  $\pm$  SEM.....60

Figure 19. MEK 1/2 inhibitor effects on organoid, luminal and myoepithelial cell morphologies. Images are a projection images constructed from a z-series captured on a confocal scope. Organoids were treated as indicated. Green images are stained with phalloidin conjugated with Alexa-488, which stained actin, and labeled all cells. Red images are stained for SMA, which is a specific marker of myoepithelial cells. Note the rounded morphology of the myoepithelial cells in U0126-treated organoids as indicated by the white arrows. (mag. 200x).....61

Figure 20. Effect of MMP inhibition on proliferation at 72hrs. A. Fold increase in proliferation determined by 3H-tdr incorporation was calculated versus BM of control treatments. An inhibitor concentration of 10 $\mu$ M GM6001 was used. B. Effect of MMP inhibition. 3H-tdr incorporation was expressed as a percentage of corresponding control treatment. Each bar = mean  $\pm$  SEM.....62

Figure 21. MMP inhibitor effects on organoid, luminal epithelial cell, and myoepithelial cell morphologies. Images are a projection images constructed from a z-series captured on a confocal microscope. Organoids were treated as indicated. Green images are stained with phalloidin conjugated with Alexa-488, which stained actin, and labeled all cells. Red images are stained for smooth muscle actin (SMA), which is a specific marker of myoepithelial cells. Note the presence only of extensions and chains of cells; cords and tubules are not present in GM6001-treated organoids. White arrows indicate chains and extensions. (mag. 200x).....63



## KEY TO SYMBOLS OR ABBEVIATIONS

17 $\beta$ -estradiol (E2)  
Basal media (BM)  
Di-methyl sulfoxide (DMSO)  
Estrogen (E)  
Estrogen receptor alpha (ER $\alpha$ )  
Extracellular matrix (ECM)  
Extra-cellular signal related kinase (ERK)  
Fluorescein (FITC)  
Glycogen synthase kinase-3 $\beta$  (GSK-3 $\beta$ )  
Hanks Balanced Salt Solution (HBSS)  
Hepatocyte growth factor (HGF)  
Hormone replacement therapy (HRT)  
Knock-out (K/O)  
Madin Darby canine kidney (MDCK)  
Matrix metalloprotease (MMP)  
Mitogen-activated protein kinase (MAPK)  
Phosphoinositide-3 kinase (PI3K)  
Progesterone (P)  
Progesterone receptor (PR)  
Progesterone receptor knock-out mice (PR K/O)  
PR A knock-out (PRA K/O)  
PR B knock-out (PRB K/O)  
Progesterone responsive element (PRE)  
SH2-containing inositol 5-phosphatase 1 (SHIP-1)  
Smooth muscle actin (SMA)  
Tritiated-thymidine (<sup>3</sup>H-tdr)  
Whey acidic protein (WAP)

## **Introduction**

### **Progesterone has Major Mitogenic Activity in the Human Adult Mammary Gland**

Progesterone (P) has a role in regulating proliferation in the human breast. Proliferation in response to estrogen (E) vs. E+P in the postmenopausal human breast of patients receiving hormone replacement therapy (HRT) has been examined (1). It was found that the proliferation index and epithelial density were greater in women receiving E+P treatment than E alone. In the same study, proliferation of breast tissue was examined during both the luteal and follicular phase of the menstrual cycle of premenopausal women. During the luteal phase when both E and P were present, proliferation indices were similar to postmenopausal women receiving E+P HRT and are greater than during the follicular phase when only E was present.

Since this report on the effect of E vs. E+P in the human breast, at least four studies of HRT's effect on breast cancer risk have shown that a greater cancer risk is associated with E+P HRT (2-5). The most recent study is the Womens' Health Initiative, a study that was stopped due to the negative effects of E+P HRT, one of which was increased breast cancer risk (5). Therefore, there is substantial evidence that P is a strong mitogen in the adult pre and postmenopausal breast and that the mitogenic activity of P can lead to an increased breast cancer risk.

### **The Mouse Model**

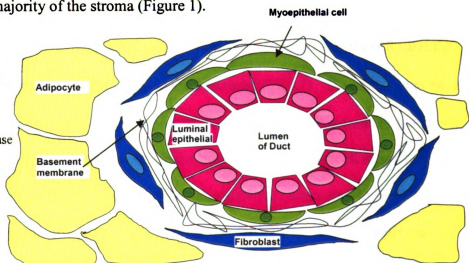
The mouse is the most extensively studied and best described model of mammary gland growth and development. Furthermore, the mouse mammary gland is similar to the human breast with regard to response to growth factors and hormones. The observation

of the greater proliferative effect of E+P in the adult human breast has also been shown to be in agreement with studies in the mouse mammary gland (6).

### **Mammary Gland Organization and the Epithelial Subtypes of the Mammary Gland**

Since the majority of the development of the mammary gland takes place postnatally, how the gland is organized is dependent on the stage of development. From birth to sexual maturity the predominant structures in the mammary gland are ducts. The duct structure consists of cuboidal epithelial cells, luminal cells, that line the lumen of the duct. Luminal epithelial cells are surrounded by a continuous layer of myoepithelial cells, a contractile cell type which run parallel to the direction of the duct. The epithelial compartment, consisting of both luminal and myoepithelial cells, is surrounded by a basement membrane consisting of extracellular matrix (ECM) proteins that are secreted predominately by the stromal cells of the mammary gland (7). In ducts the myoepithelial cells are the predominant epithelial cell type in contact with the basement membrane (8). The stroma is comprised of fibroblasts and adipocytes, as well as blood vessels, lymphoid tissue, and nerve fibers. Fibroblasts are closely associated with the epithelial compartment of the mammary gland, surrounding the ducts. The adipocytes are the cells that constitute majority of the stroma (Figure 1).

Figure 1. Diagram  
of *in vivo*  
architecture of mouse  
mammary duct.  
Figure created by  
Alexis Drolet



During pregnancy the organization of the mammary gland is greatly altered. The main structures present are alveoli organized in lobules. While the organization of the cell types is still similar with luminal epithelial cells and then myoepithelial cells both surrounded by a basement membrane, the organization of the myoepithelial cells is different. Myoepithelial cell shape is more stellate and the myoepithelial cells form a basket- or net-like structure around the lobules as opposed to laminating the luminal cells in ducts. In this arrangement the luminal epithelial cells in alveoli are allowed much greater contact with the basement membrane (8).

Luminal epithelial cells are generally thought of as the main functional cells of the mammary gland. It is in the luminal epithelial cells of the alveoli that milk is synthesized during lactation. Of the epithelial subtypes, the luminal epithelial cells have been more widely studied than myoepithelial cells. Most of the mammary epithelial cell lines used today, cancerous and normal, are of luminal epithelial cell origin. While a comprehensive review of luminal cell properties is beyond the scope of this literature review a few characteristics of luminal cells need to be mentioned. First, the luminal cells are more proliferative than the myoepithelial cells (9). Second, it is only in the luminal cells and not in myoepithelial cells that the progesterone receptor (PR) and the alpha form of the estrogen receptor (ER $\alpha$ ) are expressed (10, 11). These receptors have both been shown to be important in the normal development of the mammary gland (12, 13). Finally, the majority of carcinomas in the breast are of luminal cell origin (8).

Myoepithelial cells are highly contractile cells that contain muscle specific cytoskeletal and contractile proteins (8). However, like all true epithelial cells they

express cytokeratins, and are separated from the connective tissue by a basement membrane. Functionally, the main role of the myoepithelial cells is the ejection of milk during lactation through the action of their contractile properties. Until recently little else was known about the functions of myoepithelial cells. It is now known that myoepithelial cells are important in establishing the correct polarity of luminal epithelial cells. Luminal epithelial cells cultured in a collagen gel matrix form a fluid filled cyst. However, in the absence of myoepithelial cell the polarity of the luminal epithelial cells is reversed (14). Myoepithelial cells are also now believed to have tumor suppressive properties. mRNA expression profiles were used to compare gene expression profiles in myoepithelial cells vs. non-myoepithelial breast carcinoma cell lines and breast carcinoma samples. It was seen that the myoepithelial cell expression profile is that of a tumor suppressor, with increased expression of extra-cellular matrix proteins, angiogenesis inhibitors, and proteinase inhibitors. Decreased expression of angiogenic factors and proteinases is also seen (9). Further evidence of the tumor suppressing capabilities of myoepithelial cells is seen in the ability of myoepithelial cells to inhibit proliferation of breast cancer cell lines when they are co-cultured (15). Overall, a better understanding of mammary gland development as well as breast cancer will be achieved through the use of model systems that investigate how both epithelial cell types function together in close proximity, similar to their arrangement *in vivo*.

### **Mammary Gland Development in the Mouse**

In order to understand the role of P in the mouse mammary gland, it is important to understand the program of development in the mammary gland. In the mouse at birth, the mammary gland is a rudimentary system of simple, un-branched ducts extending

from the nipple on a background of stroma, known as the fat pad. At puberty, the epithelial cells begin to proliferate and form a tree-like pattern of ducts. The ends of the ducts exhibit bulbous tips known as end buds. It is in these end buds that the majority of cell proliferation takes place in the pubertal gland. The growth continues until the ducts fill the fat pad. At this point, the end buds regress, and the ducts become proliferatively quiescent (Figure 2).

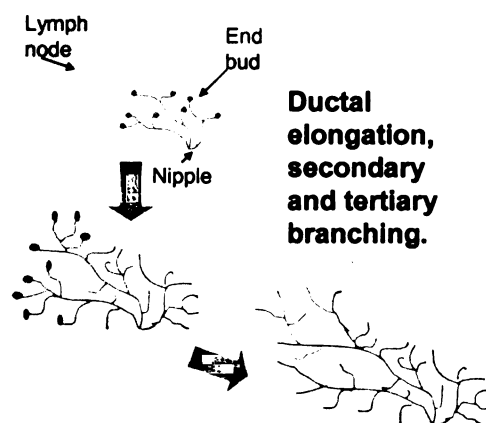
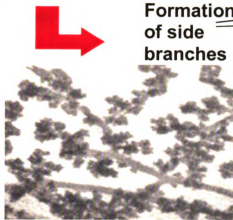


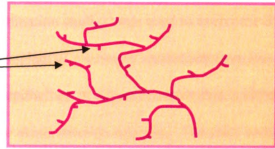
Figure 2. Development of mouse mammary gland from birth to sexual maturity. Figure created by Alexis Drolet.

The adult mammary gland shows some proliferation with each estrus cycle producing small alveoli on the lateral buds followed by regression. The onset of pregnancy again brings about high levels of proliferation in the mammary epithelium. The ducts form extensive side branches and alveoli are formed from these side branches (Figure 3). Upon parturition, the alveoli synthesize and secrete milk proteins. Epithelial cell proliferation ceases near the onset of lactation. Once lactation ceases, the glands undergo involution and return to a state similar to the pre-pregnancy state, with the exception that some alveolar structures remain.

**Early in pregnancy or hormone treatment**



**Formation of side branches**



**As pregnancy progresses**

**Ducts continue to swell and side branches develop into alveoli**



Figure 3. Development of the mouse mammary gland during pregnancy. Figure created by Alexis Drolet.

### **The Role of Progesterone in Mammary Epithelial Cell Proliferation in the Mouse**

Systemic P is not present until estrus cycles begin at puberty. The mouse estrus cycle is 4 days in length and can be divided into two separate stages, estrus and diestrus. It is during diestrus that serum levels of P increase (16). However the increase in the levels of P is not necessary for the proliferation that takes place during ductal elongation in the pubertal mouse. In progesterone receptor (PR) knock-out mice (PR K/O), which lack the receptors for P, ductal elongation occurs normally (17).

Pregnancy, the other stage in mouse mammary gland development that exhibits high levels of proliferation, is dependent on the actions of P. Serum levels of P rise well beyond the levels seen during diestrus. Since PR K/O mice are unable to undergo estrus or pregnancy because P is needed for the normal ovulatory cycle to occur, more complex techniques were needed to determine what phenotype was present in the mammary

epithelium of PR K/O mice. Tissue recombination studies were used to overcome this problem. Tissue recombination takes a transplant of mammary epithelium from one mouse and places it in a fat pad cleared of epithelium in a second mouse that is either of the same strain or immuno-compromised to avoid immune rejection. The mice receiving the transplant can then be bred and the transplanted mammary gland can be observed to determine if a phenotype is present. Using the gland transplant technique it was observed that PR-negative ductal epithelium transplanted to wild type mice is unable to form the alveolar morphology seen in response to pregnancy (13). P has also been shown to be necessary for ductal side branching that precedes alveolar formation and to be required for epithelial cell proliferation in the adult gland in response to pregnancy (13).

### **Mechanisms of Progesterone Action**

Progesterone exerts its morphologic and proliferative effects through its cognate receptor, the progesterone receptor (PR). The PR exists in two naturally occurring isoforms, PR A and PR B, which are produced from the same gene through the use of alternate start sites under the control of two separate promoters (18-20). The PR A isoform is a truncated version of the PR B form, missing the N-terminal 128-165 amino acids depending on the species (18). Both PR isoforms are functional, and able to bind P as well as alter transcription of responsive genes. Studies *in vitro* in cell lines have shown that the two isoforms exhibit different transcriptional activities (21). Gene array studies also done *in vitro* in the T47D human mammary tumor cell line showed that some genes are differentially regulated by the two PR isoforms (22).

Recent work in our lab (23) examined the developmental expression of the PR A and B isoforms in the BALB/c mouse mammary gland. PR A protein expression is



present in the virgin mammary gland as early as 3 weeks of age in nearly 50% of luminal epithelial cells. The percent of PR A positive cells does not change much through puberty and is at similar levels in the sexually mature mouse at 12 weeks of age. As the nulliparous mice age further, PR A levels show a decrease in the number of PR A positive cells to 30% of luminal epithelial cells at 17-20 weeks of age. The number of PR A positive cells then decreases dramatically during pregnancy to only 10% of luminal epithelial cells at 14 days of pregnancy. PR B is abundantly expressed only during pregnancy with 50% of luminal cells positive for PR B at 14 days of pregnancy, suggesting that expression of PR B is likely important in alveologenesis (23).

Two major mechanisms exist by which P may exert its effects within the mammary gland. First, since the PR is a class 1 nuclear family receptor, it may act as other nuclear receptors do to alter gene transcription through binding directly to specific DNA elements. Upon P binding to the PR, its association with heat shock proteins is lost and it dimerizes and translocates to the nucleus. Once in the nucleus, the PR binds the DNA through its DNA-binding domain at a specified sequence known as a progesterone responsive element (PRE), and depending on which co-activators or co-repressors are present within the cell and are present at the PRE-containing gene promoter, the PR can either up or down-regulate the transcription of a given gene (18). The changes in the expression of these genes could then mediate the action of P in the mammary gland within PR expressing cells. P has been shown to be involved in increasing the transcription of cyclin D1 and Stat 5a, both of which are important in the alveolar development of the mammary gland (22).

The PR may also alter transcription of genes whose protein product could act on adjacent PR negative cells in a paracrine fashion. The glands of total PR knock-out (PR K/O) are unable to develop normally in response to pregnancy to form alveoli. However, a study using chimeric epithelium, in which PR K/O cells were in close proximity to PR+/+ cells, the reconstituted mammary gland was able to develop normally, both proliferatively and morphologically, in response to pregnancy (13). Therefore, P may also act on PR expressing cells to induce paracrine factors that act on cells that are not expressing PR.

The role of phosphorylation of PR protein residues has been examined recently. Studies in the T47D human mammary cancer cell line have shown that PR is phosphorylated on Ser294 in response to both progestin treatment and in response to MAPK (p42 and p44) activation resulting from growth factor stimulation (24). Phosphorylation at Ser294 by growth factors was shown to have three major effects: 1) it enhanced PR nuclear localization, 2) it mediated transcriptional synergy with progestins on PRE-luciferase construct, and 3) it was essential for rapid turnover of liganded PR. These effects were abrogated if cells were treated with inhibitors of MEK 1/2 or if a construct with a Serine to Alanine mutation was used (24). These results indicate that the actions of P through the PR may also be influenced or altered by the growth factor signaling environment present within a given cell.

The second mechanism in which P may exert its effects through the PR is through a direct interaction between the PR and other signaling intermediates. Evidence for a direct action of PR on signaling proteins is found in a report by Edwards, et al. (25). They showed that both isoforms of PR, PR A and B, contain a SH3 binding domain,

whose binding activity is dependent on P binding to the receptor. This domain has been shown to bind and activate Src as well as other SH3-containing signaling proteins in response to P (25). It is plausible that this SH3-binding domain may also bind with other SH3-containing proteins other than Src to exert the effects of P. This mechanism of action would be confined solely to the specific cell types that are expressing PR. In summary, it is likely that P may act through both nuclear and cytoplasmic signaling in order to exert its effects.

### **Knock-out Studies and Progesterone Action**

Knock-out (K/O) mice have been generated for a number of different proteins to examine their roles in the development of the mammary gland as well as other tissues. Studies on the total PR K/O mice, lacking both isoforms, have shown that when PR is lost the mammary gland does not respond to P-treatment and fails to form side-branches and alveoli in gland transplantation studies (17). More recent studies looked at the single isoform knock-outs. The PR A knock-out (PRA K/O) mouse exhibits normal development of the mammary gland throughout development; ductal elongation during puberty and alveologenesis during pregnancy both appear normal (26). The PR B knock-out (PRB K/O) mouse also exhibits normal pubertal development with no effect seen on ductal elongation. However, in response to pregnancy the mammary gland of the PRB K/O mice are unable to form alveoli or lactate (27).

The PR K/O mouse mammary glands are able to form normal ducts during puberty but are unable to proliferate, form side-branches, or form alveoli in response to treatment with estrogen and progesterone (17). This finding suggests that P is essential for the gland to form side branches as well as to form alveoli. The mechanism of P

action, as described previously, is to alter levels or activation of other proteins in order to exert its effects. It is logical to presume that if a P-induced protein mediating the effect of P were to be knocked out, the resulting phenotype in the mouse mammary gland would be very similar to the PR knock-out phenotype. This hypothesis has led to the identification of some possible target proteins that are essential for P action in the mammary gland.

Wnt-4 is a secreted glycoprotein that is a member of the Wnt protein family. Wnt proteins are involved in embryological development during axis formation; however, they are also known to play a role in organ and tissue formation (28). A knock-out of Wnt-4 is embryonic lethal in mice, but through the use of mammary gland reconstitution techniques, Briskin et al. was able to take Wnt-4 K/O mammary epithelium from the embryonic mammary gland and place it in the cleared fat pad of a normal mouse to produce a Wnt-4 K/O mammary gland. The Wnt-4 K/O mammary glands are able to develop normally through sexual maturity. However, the glands are unable to form the side-branches normally seen in early pregnancy, similar to the phenotype of the PR K/O mouse. Despite this, by late pregnancy the Wnt-4 K/O glands are able to form normal lactating glands. The proposed explanation was that other wnt proteins expressed in late pregnancy are able to replace Wnt-4 to recover the normal phenotype (29). Briskin also showed that Wnt-4 is the only member of the wnt family that is regulated by P. Treatment of mammary epithelial cells with P led to an increase in Wnt-4 mRNA expression (29). These results suggest that Wnt-4 mediates side branching in early pregnancy.

Cyclin D1 K/O mice also exhibit a mammary phenotype very similar to that of the PR K/O (30). The glands are able to develop normally during puberty through sexual maturity. However, in response to pregnancy the gland is unable to form alveoli and lactate, suggesting that cyclin D1 is an essential mediator of P action in the mammary gland. Further supporting this hypothesis is the data that gene deletion or inhibition of proteins involved in associating with, activating, and maintaining cyclin D1 expression, such as P27,  $\beta$ -catenin, and Pin 1 respectively, all exhibit phenotypes similar to the cyclin D1 K/O (31-33).

Other K/Os, such as C/EBP $\beta$  and Stat 5a, also exhibit phenotypes similar to that of the PR K/O (34, 35). Stat 5a K/O mice are unable to form functional alveoli in response to pregnancy, which is also true of the PR K/O. However, the inability of the Stat5a KO to form functional alveoli is not due to the lack of lobuloalveolar structures, but most likely due to a lack of functional differentiation of the alveolar epithelium (35). The C/EBP $\beta$  K/O mouse also exhibits a lack of functional alveoli in the mammary gland. The mammary glands of the C/EBP $\beta$  K/O mouse also exhibit altered expression of the PR protein. Normally, PR is expressed in about 40% of luminal cells in a spotty or punctuate pattern. In the C/EBP $\beta$  K/O mammary gland the expression pattern of PR is uniform, with PR expressed in almost all the luminal cells. Since it is not known which PR isoforms are effected within the C/EBP $\beta$  K/O, it is presently difficult to interpret the role of PR in the resultant phenotype (34). Overall, these studies show that many proteins are essential for normal P-mediated actions to occur during mammary gland development.

## **Stromal Cell Influences on Mammary Gland Development**

Our lab and others have shown that the proliferative and morphological response of the mammary epithelium to E and P is dependent upon epithelial cell-stromal cell interactions (36). Using a primary culture system, we and others were able to determine that a growth factor is produced by stromal cells. Epithelial organoids co-cultured with mammary fibroblasts will proliferate and form tubules. This response is also seen when epithelial organoids are treated with fibroblast- conditioned media. Through the use of neutralizing antibody experiments our lab determined that hepatocyte growth factor (HGF) is the factor responsible for the proliferative and morphologic effects.

### **Hepatocyte Growth Factor and its Receptor, c-Met**

Hepatocyte growth factor, which was originally identified and cloned as a potent mitogen for hepatocytes, has been shown to have both biological and physiological roles in development and in tissue regeneration of various different organs and tissues (37). Hepatocyte growth factor is composed of an  $\alpha$ -chain, which contains a NH<sub>2</sub>-terminal hairpin and four kringle domains, and the catalytically inactive serine protease-like  $\beta$ -chain (38). Hepatocyte growth factor is produced only by fibroblasts in the mammary gland and this production is developmentally regulated (39). Its expression is first seen during puberty at around 5 weeks of age in the mouse. Maximal expression occurs at 12 weeks of age in the mouse, at sexual maturity, and this is also the time when the mammary gland will respond to P by forming ductal side branches and alveoli. Expression of HGF is lost in late pregnancy and lactation (39, 40).

The receptor for HGF, c-Met, is expressed only in the epithelial compartment of the mammary gland. c-Met is a 190 kDa protein tyrosine kinase, consisting of a 50 kDa

extra-cellular domain, which is responsible for its ligand binding function, and a 145 kDa transmembrane/cytoplasmic domain, containing the kinase activity (41). Upon binding of HGF to c-Met, autophosphorylation of the cytoplasmic tail is seen at a number of tyrosine residues. These phosphorylated residues provide a binding site for a number of signaling proteins containing a SRC homology 2 domain (SH2) or a phosphotyrosine binding domain (41). The adapter proteins Gab1, GRB2, the p85 subunit of phosphoinositide-3 kinase (PI3K), Src, Shc and the SH2-containing inositol 5-phosphatase (SHIP)-1 all have the ability to bind to c-Met and can recruit and activate a number of signaling pathways (41). Depending on which signaling pathways are activated in response to HGF, mitogenic, morphogenic, and motogenic responses are seen in many cell types including mammary epithelial cells (42).

However, a discrepancy exists in the literature as to the expression of the HGF receptor, c-Met. One study using a Northern blot assay shows that c-Met follows the same pattern of expression as HGF (39). A second study using an RNase protection assay shows c-Met increasing through puberty and no down-regulation of c-Met during late pregnancy or lactation (40). Both the HGF and c-Met expression studies were done using RNA from homogenized glandular tissue, so little is known about the relative expression of the c-Met protein in the luminal vs. myoepithelial cells of the mammary gland.

In a study using human primary cultures of purified luminal or myoepithelial cells, both cell types were shown to express c-Met and exhibited distinct responses to HGF. While both cell types showed a motogenic response to HGF, myoepithelial cells exhibited a morphogenic (tubulogenic) response as well, but no mitogenic response was

seen. In contrast, a mitogenic response was observed only in luminal epithelial cells, but no morphogenic response was observed (39). It is possible that HGF may act through c-Met to initiate different pathways within these two different cell types.

Hepatocyte growth factor has been shown to be necessary for branching morphogenesis in the mammary gland. A study using anti-sense oligonucleotides against HGF showed that branching morphogenesis is blocked in whole mammary gland cultures (40). Work in our lab has also addressed the role of HGF-induced branching morphogenesis *in vivo*. Elvax pellets containing a neutralizing antibody to HGF are able to block side-branching induced by an adjacent pellet containing E+P or induced by systemic E+P injection (43). Transgenic mice in which HGF was targeted to the mammary epithelium by the whey acidic protein (WAP) promoter have been generated to examine the role of HGF in breast cancer (44). Results from this study also shed some light on the role of HGF in mammary gland development. In virgin females, overexpression of HGF in the mammary epithelium leads to the formation of lobular structures protruding off of ducts. However, in the presence of the unscheduled HGF expression, lactation is able to occur normally. Since the WAP promoter is induced during pregnancy, multiple pregnancies led the female mice to develop hyperplastic ductal trees and invasive tumors in response to HGF overexpression. It was observed in these tumors that the levels of active AKT and nuclear  $\beta$ -catenin were elevated.

### **Models of HGF-induced Tubulogenesis**

Until recently, the manner in which groups or cysts of cells formed tubules has not been well understood. Two competing hypotheses now exist. The first from work done in Madin Darby canine kidney (MDCK) cells, argues that the formation of tubules



is the culmination of a four-step process (45). First, in response to a stimulus, such as HGF, a cell will form an extension, that is an elongated section of the cell projecting out from the main group of cells. Once the extension is formed the following steps require proliferation to occur. Proliferation of the cell that forms the extension leads to the formation of a chain of cells. Further proliferation allows for the formation of a cord, which is comprised of two layers of cells with a discontinuous lumen. This is finally followed by reorganization of the two layers of cells to form a continuous lumen, which constitutes a tubule.

Further work by the Mostov lab has also shown that in order for formation of extensions and chains of cells to occur extra-cellular signal related kinase (ERK) activity must be present. When ERK 1/2 signaling was blocked, formation of extensions and chains was lost (46). The same study also showed that matrix metalloprotease (MMP) activity was needed for chains of cells to further progress into cords and tubules. When MMP activity was inhibited, the cysts of MDCK cells were only able to form extensions and chains of cells in response to HGF.

The second hypothesis was also generated from work done in MDCK cells and suggests that tubule formation is a two step process. The first step is the loosening of the lateral membranes and the formation of large paracellular spaces. The second step is then the formation of basal protrusions of more than one cell, which then continue extending to form new tubules. In this model there is always a continuous lumen present (47). The authors of this paper suggest strain differences in MDCK cells and the use of mouse recombinant HGF as possible reasons for the differing mechanisms of tubule formation

reported using the MDCK cell line. However, they felt these explanations could not adequately explain the differing mechanisms observed and did not speculate any further.

### **An *In Vitro* Model to Study Progesterone-Induced Proliferation**

Much has been learned from the studies of normal, knock-out, and transgenic animals *in vivo*; however, the complexity of the mammary gland, with its various cell types and growth factors, has made it difficult to interpret the function of specific factors in the mammary gland. Understanding the mechanisms of P-induced proliferation in the mammary gland has been hampered by the lack of a good, *in vitro*, experimental model. An appropriate cell culture system can overcome these problems. There is no normal, non-transformed human or rodent cell line that expresses both ER and PR and exhibits a mitogenic response to P. Many studies have used a primary culture system. However, most studies were carried out in the presence of serum, impure supplements and/or high concentrations of insulin, which can act like insulin-like growth factor I, a potent mitogen in the mammary gland. The use of these factors in experiments can confound results. The use of extracellular matrix gel preparations (matrigel, collagen I) have allowed mammary epithelial cells to grow into three dimensional structures which more closely resemble their structure *in vivo* and provide a more physiological context in which to study growth and morphogenesis. For these reasons, investigators are more frequently using a three dimensional culture systems and serum free media.

Our lab has developed a serum-free, 3-D (collagen gel) primary culture system using mammary epithelial cell organoids from adult virgin mice, which expresses both ER and PR. Importantly, P induces proliferation and an alveolar-like morphogenesis in this system, similar to the P-induced responses seen *in vivo*. To the best of our

knowledge, this is the first report of a mitogenic and morphologic response to P *in vitro* under defined, serum-free conditions that simulates the responses to P seen *in vivo*.

For P-induced proliferation and morphogenesis to occur in our *in vitro* system, the presence of HGF is required. After 3 days in culture, the synthetic progestin, R5020, when added with HGF caused an 8-fold increase in proliferation over control cultures and a significant 1.5-fold increase over cultures treated with HGF alone (Figure 4).

Interestingly, the morphogenic response to R5020+HGF resembles the alveologenic response seen *in vivo* in response to P (Figure 5). In contrast, treatment with HGF alone increases proliferation and produces a tubulogenic response, similar to that seen during ductal elongation *in vivo*. While treatment with R5020 alone had no proliferative effect, lumen formation was observed (Figures. 4 and 5). Since P cannot act independently of HGF to increase proliferation or induce an alveolar-like morphology, it implies that there must be interactions between P and the HGF signaling pathways.

Another important aspect of our culture model is that our isolation procedures give us organoids consisting of both luminal epithelial and myoepithelial cells. This is important because both cell types are found in the ducts of the mammary gland and participate in morphogenesis *in vivo*. Studies have also shown that luminal epithelial and myoepithelial cells when cultured separately will respond differently to HGF (39), and that normal polarity of luminal cells is reversed (14).

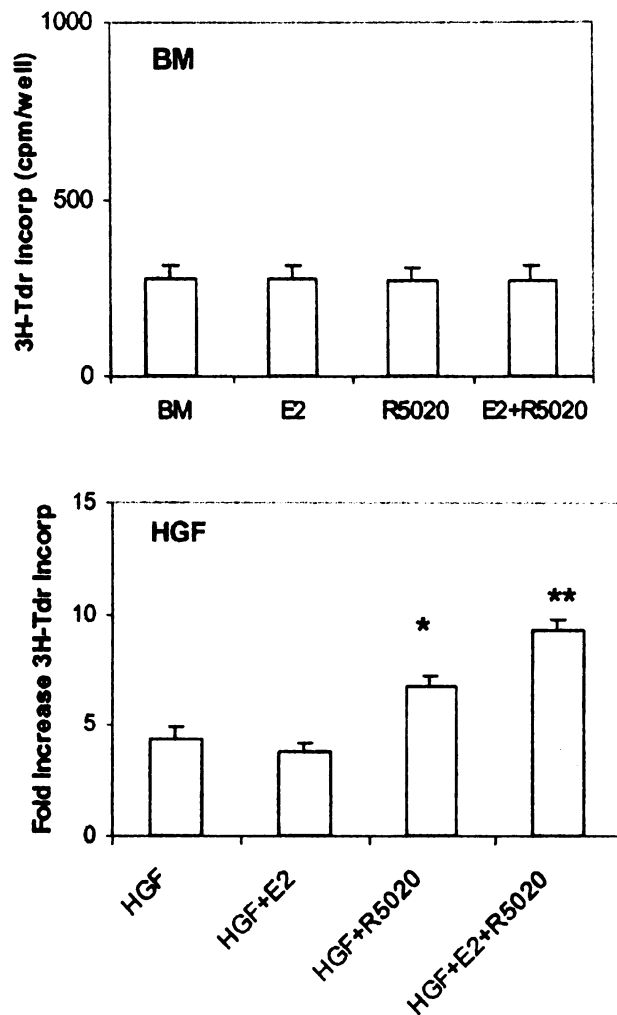


Figure 4. Effect of progestin (R5020) on epithelial cell proliferation in collagen gels. Mammary epithelial cells in collagen gels were cultured alone (BM+Hormones) or with HGF (50ng/ml). For each of these conditions cells also received treatment with basal media only (BM), Estradiol 20nM (E2), R5020 10nM, or E2+R5020 (20nM+10nM). 3H-thymidine incorporation was assayed on day 3. The data are expressed as fold increases over basal media. Each bar= mean  $\pm$  S.E.M. of triplicate determination from 3-5 separate experiments. \*  $p=0.05$  that proliferation in HGF+R5020 treated cultures is greater than HGF and HGF+E2-treated cultures within each treatment group. \*\*  $p=0.05$  that proliferation in HGF+E2+R5020 is

greater than all other treatments within each treatment group. Endocrinology Vol. 143, No. 8 2953-2960.

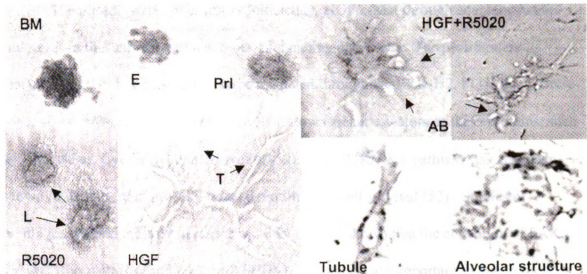


Figure 5. Phase contrast photomicrographs of epithelial cell organoid morphology in collagen gel cell culture. Mammary epithelial cells were suspended in collagen I gels and cultured for 3 d in BM, E2, PRL (1  $\mu$ g/ml), R5020, HGF, or R5020+HGF. Gross organoid morphology was visualized *in situ* in collagen gels with the aid of an inverted microscope (magnification, x100) and in histological sections of collagen gels (magnification, x400). Organoids appear solid when treated with BM, E2, and PRL, whereas lumens (L), tubules (T), and alveolar buds (AB) are visible in R5020, HGF, and R5020 plus HGF cultures, respectively. Sections through a tubule and alveolar structure are also shown. *Endocrinology* Vol. 143, No. 8 2953-2960.

### **Signaling Pathways Relevant to Proliferation, Morphogenesis, and Interactions between HGF and Progesterone**

Immunohistochemical and *in situ* hybridization studies of luminal epithelial cells have shown them to contain PR; *in situ* hybridization assays have shown that myoepithelial cells do not express PR (10). Three dimensional mammary organoid cultures treated with HGF alone show a tubulogenic response, while cultures treated with both HGF and R5020 show an alveolar-like response. This response could be the result of 1) a direct interaction of the PR on HGF signaling through binding of the PR to an HGF downstream effector or 2) an indirect interaction via a paracrine factor induced by R5020 in PR positive epithelial cells that interacts to alter HGF signaling in PR negative luminal epithelial and/or myoepithelial cells.

The phosphorylation cascades initiated by HGF/c-Met through adapter proteins can result in the activation of a number of signaling pathways. The proliferative response to HGF has been shown to be mediated through the ERK 1/2, PI3K/AKT, Src/c-Myc, and wnt/ $\beta$ -catenin pathways as well as downstream effectors of these proteins, such as JNK, c-Fos, Cyclin D1, and c-Myc (48-52). The PI3K/AKT pathway has also been shown to be important in HGF induced motility and cell survival (52). Studies of tubulogenesis and motility in responses to HGF have shown that the activation of FAK, the Rac/Rho pathway, and the Grb-2/SHIP-1/2 pathways are important to due to their involvement in cell adhesion and cytoskeletal organization (53). The Wnt-4 pathway has also been shown to be important in P-induced side-branching seen during pregnancy *in vivo* (29). It has also been shown in human mammary epithelial cells in culture that an increase of wnt proteins precedes a decrease in the HGF-induced tubulogenic response (54). This could indicate a role for wnt protein in the response of organoids to HGF+R5020, which exhibit blunted tubules when compared to HGF treatment.  $\beta$ -catenin is activated in response to HGF treatment and is part of the E-cadherin complexes involved in tubulogenic response of HGF (45).

Many of these studies have been carried out *in vitro* in a variety of cell types under various culture conditions. However, little is known about which pathways are activated by HGF in the normal mammary gland. Some individual pathways have been investigated in normal mammary epithelial and breast cancer cell lines in response to HGF treatment. In the case of proliferation, the ERK 1/2 and PI3K/AKT pathways are activated (51, 52). Tubulogenesis studies have implicated the FAK and PI3K/AKT pathways (55, 56). It is possible that some pathways, such as PI3K/AKT, may

function in both responses. Knockout studies have shown that Wnt-4 and cyclin D1 are essential for side branching and alveolar formation during early pregnancy, respectively (29, 30).

### **Matrix Metalloproteinases (MMPs) and Mammary Development**

Matrix metalloproteinases are important in the tubulogenic response to HGF treatment in MDCK cells. It has been shown that MMP activity is also important in mouse mammary gland development. Studies looking at specific MMPs in mammary gland development have shown that MMP2 is important for ductal elongation and when knocked out it results in delayed ductal elongation and increased side branching in the pubertal gland. In contrast, loss of MMP3 led to delayed side branching during early pregnancy (57). Earlier work looking at a transgenic mouse over expressing MMP3 showed excessive side branching in the virgin gland and that MMP3 can act as a mammary tumor promoter (58, 59). The authors of the MMP3 transgenic studies propose a model in which MMP3 could lead to increased proliferation. In this model MMP3 would cleave E-cadherin in luminal epithelial cells, releasing  $\beta$ -catenin from the cadherin complexes and increasing its cytosolic levels;  $\beta$ -catenin could then translocate to the nucleus where it partners with TCF/LEF transcription factors to lead to increased expression of responsive genes, such as cyclin D1 and c-Myc (59).

Since MMPs have a role in normal *in vivo* mammary gland development, it is likely that MMP activity may be important in culture responses involving tubulogenesis. In a mouse mammary primary culture system HGF led to increased expression of a number of MMPs (60). However, it is unclear which cells were producing the MMPs. It was previously thought that only stromal fibroblasts and possibly myoepithelial cells

were capable of secreting MMPs. A study done in a rat mammary epithelial organoid system has challenged this assumption. It was observed that rat mammary organoids were capable of producing MMPs and that pro- and anti-lactogenic hormones regulated their expression. Most interesting was the observation that P led to an up-regulation of epithelial MMP expression (61). However, in this study it was unclear which cell epithelial subtype was synthesizing the MMPs since the authors did not determine which cell types were present in their organoids. It is therefore possible that MMPs are involved in the mammary epithelial organoid response to HGF+R5020 treatment.

### **Hypothesis**

Since HGF is required for the proliferative and morphological responses to R5020, this directed us to analyze how R5020 may affect c-Met activated signaling pathways that mediate proliferation and tubulogenesis. Luminal epithelial and myoepithelial cells express c-Met, but, only luminal epithelial cells have been shown to express the PR (10). Since the luminal and myoepithelial cells express a different subset of receptors it is likely that the responses to HGF+R5020 may be specific to cell type. First we characterized the organoid system by examining cell type specific proliferation and by examining the roles of luminal and myoepithelial cells in morphology change through the use of an *in situ* antibody labeling technique. Next we asked how R5020 acts on luminal and myoepithelial cells to alter HGF responses and to determine which signaling pathways are needed in order to increase proliferation and cause a morphology change from a tubulogenic to an alveolar-like morphology in response to HGF+R5020 treatment. In order to address this question we examined cell type specific c-Met protein expression in our culture organoids under the different treatments that induce these



changes. Cell type specific c-Met protein expression was also analyzed *in vivo* to determine how similar the *in vitro* organoid system was with respect to c-Met protein expression. Since cyclin D1 is essential for alveologenesis *in vivo*, we also examined cyclin D1 protein expression under treatments that induce an alveolar-like response. Through the use of signaling pathway inhibitors, we investigated the roles of PI3K/AKT, ERK1/2, and MMPs in organoid responses to HGF and HGF+R5020. .

## **Methods**

### **Animals**

Female adult (12-20-week-old) Balb/c mice from our own colony were the source of mammary organoids for all experiments with the exception of the c-Met developmental expression studies. For the *in vivo* C-met developmental expression study the developmental stages of puberty (5wks), sexual maturity (12-16wks), pregnancy (14d), and lactation (7d) were examined.

### **Cell Culture**

Mammary epithelial organoids were isolated from whole mammary glands of adult virgin (12- to 20-wk-old) female mice using enzymatic dissociation methods as previously described (62). Briefly, mouse mammary glands were excised, minced, and digested in collagenase (Worthington, Lakewood, NJ) and pronase (Calbiochem, San Diego, CA) solutions. This was then followed by differential centrifugation and Percoll (Amersham Biosciences, Piscataway, NJ) gradient sedimentation to remove mammary stromal cells and to obtain mammary epithelial organoids consisting of both luminal and myoepithelial cells. Cell viability was about 95% as determined by trypan blue exclusion. 96-well culture dishes were coated with neutralized collagen I (2 mg/ml 40ul/well) prior to plating organoids. Freshly isolated organoids ( $1 \times 10^5$  cells /well) were suspended in neutralized collagen I (2 mg/ml, 75  $\mu$ l/well) and plated in 96-well culture dishes, and allowed to gel for 30 minutes at 37 C. All cultures were carried out in serum-free medium with or without growth factors or hormones (basal medium: serum- and phenol red-free DMEM/F12 supplemented with 0.1 mM nonessential amino acids, 2 mM L-glutamine, 100 ng/ml insulin, 1 mg/ml fatty acid-free BSA (fraction V), 100

µg/ml penicillin, and 50 µg/ml streptomycin.) Treatments with growth factors and hormones were added at the time of plating and included 50 ng/ml HGF, 10 nM E2, and 20 nM of the synthetic progestin, promogestone (R5020). R5020 was used instead of progesterone due to its better stability in culture. Cultures were kept in 5% CO<sub>2</sub> at 37 C for 3 days and culture media was replaced every 48 hrs.

### ***In Situ* Antibody Labeling of Mammary Organoids in Collagen Gels**

At various times of treatment the collagen gels containing the mammary epithelial organoids were removed with forceps and rinsed 10 minutes in phosphate buffered saline (PBS) pH 7.2 containing 1mM CaCl<sub>2</sub> and 0.5mM MgCl<sub>2</sub> (PBS+). All steps were carried out at room temperature on a rocker (Reliable Scientific, Mount Prospect, IL) at speed 4 unless otherwise noted. The gels were then fixed in 4% paraformaldehyde in PBS+. Following fixation the gels were permeabilized for 30 minutes in 0.025% saponin in PBS+. Gels were again rinsed in PBS+ for 10 minutes. This was followed quenching for 10 minutes in PBS+ containing 75mM NH<sub>4</sub>Cl and 20mM glycine. Gels were then incubated in blocking buffer consisting of 0.025% saponin in PBS+ with 0.3% gelatin for 10 minutes. Gels were then rocked at speed 4 at 4°C for 3 days in primary antibodies. Five to ten units of Alexa-488- conjugated phalloxin (Molecular Probes, Carlsbad, CA) (approximately 25 to 50 µl of methanolic stock solution) were added per ml of blocking solution. Anti-SMA (Sigma, St. Louis, MO) antibody was added at 1:200 dilution in blocking buffer. Samples then were washed 4 times in 0.025% saponin in PBS+ for 15 minutes each and washed 1x for 15 minutes in blocking buffer. Samples were incubated overnight in 1:100 dilution of goat anti-mouse Alexa 546 (Molecular Probes) and 5mg/ml TO-PRO (Molecular Probes, Carlsbad, CA) at 1:1000 dilution in Blocking buffer on a

rocker at speed 4 at 4°C. Samples then were washed 4x in 0.025% saponin in PBS+ for 15 minutes. Samples were then post fixed in 4% paraformaldehyde in 0.1M cacodylate buffer pH 7.2 and mounted on glass slides.

Images were captured using a Pascal laser scanning confocal microscope. Three separate tracks were used for capturing images: a 488 laser with 500-530 band pass filter, a 546 laser with a 580-620 band pass filter, and a 633 laser with 650 long pass filter. The images were captured in a Z-stack with average step size of approximately 4-5 $\mu$ M. Images from the Z-stack were then over-layed to create a projection image of the entire organoid.

### **Immunohistochemistry**

Gels containing organoids were fixed in 10% buffered formalin for 1 hr and then processed on the Tissue-mat (Fisher Scientific, Vernon Hills, IL) and embedded in paraffin. In the case of tissue, inguinal mammary glands were removed and fixed overnight in 10% buffered formalin and processed on the Tissue-mat (Fisher Scientific, Vernon Hills, IL) and embedded in paraffin for the *in vivo* c-Met studies. Five  $\mu$ m paraffin embedded sections were placed on coverslips treated with (3-Aminopropyl) triethoxy-silane (APES), deparaffinized, and subjected to antigen retrieval by autoclaving in citrate buffer as previously described (63). Sections were blocked with goat anti-mouse IgG Fab (Jackson Laboratories, Bar Harbor, ME) 1:100 dilution in 1% bovine serum albumin (BSA) in PBS followed by normal goat serum (Vector Labs, Burlingame, CA). The sections were then incubated with mouse monoclonal antibodies to either PRA (hPRa7) 1:100 dilution, PRB (hPRa6) 1:100 dilution, cyclin D1 (Cell Signaling Technology, Beverly, MA) 1:100 dilution, alpha smooth muscle actin (Sigma, St. Louis,

MO) 1:400 dilution, bromo-deoxyuridine (BrdU) (Amersham Biosciences, Piscataway, NJ) undiluted or rabbit polyclonal antibody to Met (Santa Cruz Biotechnology, Santa Cruz, CA) 1:50 dilution. Sections were then incubated with goat anti-mouse or goat anti-rabbit conjugated Alexa 488 or Alexa 546 (Molecular Probes, Carlsbad, CA), both 1:100 dilutions, and mounted with fluorescent mounting media containing a 1:1000 dilution of the nuclear stain TO-PRO®-3 iodide (Molecular Probes, Carlsbad, CA).

Fluorescent images were captured using a Pascal laser scanning confocal microscope. Three separate tracks were used for capturing images: a 488 laser with 500-530 band pass filter, a 546 laser with a 580-620 band pass filter, and a 633 laser with 650 long pass filter.

### **Determination of proliferation in primary organoid cultures**

#### **[<sup>3</sup>H]Thymidine incorporation assay**

After 42 hrs or 66 hrs of treatment, cells were incubated with 0.1  $\mu$ Ci/well [<sup>3</sup>H]-thymidine (specific activity, 50 Ci/mmol; ICN Pharmaceuticals, Inc., Irvine, CA) at 37°C for 6 hrs. Collagen gels containing organoids were dissolved with 3.5 mM acetic acid, and transferred to GF/C filters (Whatman, Clifton, NJ), followed by washing with Hank's balanced salt solution (HBSS), ice-cold 10% trichloroacetic acid, and 90% ethanol. Radioactivity was determined by liquid scintillation counting in a Beckman Coulter LS6500 scintillation counter.

#### **BrdU Incorporation and Analysis of Cell Type Specific Proliferation**

Cultures were incubated with 10mM BrdU for 20 hrs prior to fixing gels. Formalin fixed, paraffin embedded, organoid sections were double labeled for BrdU and smooth muscle actin (SMA), and treated with 4'-6-Diamidino-2-phenylindole (DAPI) to

stain the nuclei. Using an overlay image of all three images, cells were determined to be either luminal epithelial (not expressing SMA) or myoepithelial cells (expressing SMA). Cells that were labeled for both BrdU and SMA were determined to be proliferating myoepithelial cells and cell that were labeled for BrdU only were determined to be proliferating luminal epithelial cells. Values were then tabulated and expressed as average number of BrdU positive luminal or myoepithelial cells per organoid section.

## **Immunohistochemistry Quantitation Methods**

### General Criteria for Quantitation

Two criteria were required for quantitation. First, in order for a cell to be positive for a nuclear protein at least half of the nucleus needed to be positively labeled. Second, for an image to be used for quantitation the organoid needed to contain at least 10 total cells.

### PR Isoform Quantitation

Organoids stained for either PR A or PR B were quantitated for number of positive cells and total number of cells. This allowed the determination of the percentage of the cells that were PRA or PR B positive.

### C-met Quantitation

Organoids were stained for both C-met and SMA. The cell type was then determined by overlaying the C-met image with the SMA image. SMA expressing cells were determined to be myoepithelial cells and were quantitated separately from luminal epithelial cells. Images were captured using laser scanning confocal microscopy and were then analyzed by measuring the mean Alexa 488 (green) fluorescence intensity per cell. This was done by separating the Alexa 488 channel from an overlay image and then

converting it to grayscale. The average grayscale value per cell was then measured using the Image-1 program.

#### Cyclin D1 Quantitation

Organoids labeled for cyclin D1 were quantitated for number of D1 positive nuclei and total number of cells. Cells that showed nuclear expression of cyclin D1 were considered positive if at least half of the nucleus was labeled for cyclin D1. Cells that were negative for cyclin D1 were also counted. The number of positive nuclei was then divided by the total number of cells and multiplied by 100 to determine the percent of positive nuclei for cyclin D1.

#### **Inhibitor Studies**

All inhibitors were dissolved in di-methyl sulfoxide (DMSO). Final concentration of DMSO in all control and inhibitor containing media was 0.1%. Inhibitors were added at time zero at the following concentrations: the PI3K inhibitor (LY294002 at 5 $\mu$ M) (Cell Signaling Technology, Beverly, MA), the AKT inhibitor (AKT inhibitor IV (CalBiochem, San Diego, CA) at 400nM), the MEK 1/2 inhibitor (U0126 at 10 $\mu$ M) (Cell Signaling Technology, Beverly, MA), and the broad spectrum matrix metalloproteinase inhibitor(GM6001 at 10 $\mu$ M) (CalBiochem, San Diego, CA). Culture media were replaced every 48 hrs. Organoid morphology was observed at 24, 48, and 72 hrs by phase microscopy. *In situ* antibody labeling was performed at 72 hrs in the AKT inhibitor IV-, U0126-, and GM6001-treated cultures. *In situ* antibody labeling was performed at 24, 48, and 72 hrs in the LY294002-treated cultures. Tritiated thymidine assays were performed at 48 and 72 hrs in all cultures.

## **Cell Viability Staining**

Media in wells containing organoids was removed and wells were washed one time with Hanks Balanced Salt Solution (HBSS) before adding viability dyes. Two viability dyes were used to test the viability of epithelial organoids in response to signaling inhibitors. The live cell dye, Calcein Blue 50 $\mu$ M (Molecular Probes, Carlsbad, CA) and the dead cell dye, Sytox Green 1 $\mu$ M (Molecular Probes, Carlsbad, CA) were combined in a 0.85% saline solution and 75 $\mu$ L of this solution was added per well. The plate was then incubated for 30 minutes in 5% CO<sub>2</sub> at 37 C. Results were imaged on an epi-fluorescence scope with filters for Fluorescein (FITC) and DAPI. Viability was determined by comparing the number of dead cells fluorescing (green) in inhibitor-treated vs. control-treated cultures on a grading system of 0-3, with 0 being no dead cells and 3 being 50% dead cells. Live cell dye was used to determine the size of each organoid and to determine where the dead cells were localized.



## **Results**

Images in this thesis are presented in color.

### **The Roles of Luminal Epithelial and Myoepithelial Cells in Mammary Organoids**

#### **Morphology**

Immunocytochemical methods were adapted from O'Brien et al. (46) to examine intact mammary epithelial organoids *in situ* directly in the collagen gels, in order to gain a better understanding of the roles of luminal and myoepithelial cells in morphology change in response to the various culture treatments. To accomplish this organoids were incubated with a phalloidin conjugated fluorophore, which labels actin in all cells, and a smooth muscle actin antibody (SMA), which is a specific marker of myoepithelial cells. This allowed the determination of the location and morphology of the myoepithelial and luminal epithelial cells; the latter were assumed to be the non-SMA expressing cells within the culture organoids.

As seen in figure 6, at 72 hrs organoids treated with BM showed both luminal and myoepithelial cells in a group with the myoepithelial cells exterior to the luminal cells. In response to HGF treatment the myoepithelial cells became elongated and were present mainly in the tubules branching off the organoids. Luminal cells were present both in the tubules and in the main body of organoids. R5020 treatment resulted in the myoepithelial cells external to and surrounding luminal cells, which had formed cyst-like structures. This organization was strikingly similar to mammary ducts *in vivo*, where luminal cells are surrounded basally by a layer of myoepithelial cells. HGF+R5020 treatment resulted in elongated myoepithelial cells in the tubules, and more myoepithelial cells were present

in the main body of the organoids. The luminal cells were present both in the extensions/tubules and in the main body of the organoid.

A time course of in situ labeling at 24, 48, and 72 hrs was done to examine luminal and myoepithelial cells in the mammary organoids in response to HGF to determine what role each cell type was playing in the formation tubules (Figure 7). Twenty-four hours of HGF treatment led to the formation of cellular extensions from cells within the organoid, and these extensions consisted of mostly luminal cells. After 48 hrs of HGF treatment the extensions were longer and some chains of cells were present. SMA expressing cells were now present in the extensions and chains but did not appear to be at the leading edge of either. At 72 hrs of HGF treatment the myoepithelial cells were elongated and were present mainly in the extensions/tubules branching off the organoids. Luminal cells were present both in the extensions/tubules and in the main body of the organoids.

### **Cell Type Specific Proliferation *In Vitro***

Since cultured organoids contained both luminal and myoepithelial cells, it was necessary to identify the cell type that was proliferating under HGF versus HGF + R5020 treatment. This question was addressed by antibody double labeling of culture organoids for SMA and for the proliferation indicator BrdU. Cells were determined to be myoepithelial cells if SMA expression was present. Luminal epithelial cells were identified as the cells which did not express SMA.

Shown in figure 8A is immunofluorescence staining of SMA protein expression and the proliferation marker, BrdU, for representative organoid sections treated with HGF or HGF+R5020. In the HGF-treated organoids no BrdU labeling was seen in SMA

positive cells but was seen in luminal cells. HGF+R5020-treated organoids exhibited BrdU labeling of both SMA positive (myoepithelial) and negative (luminal epithelial) cells. Figure 8B shows quantitation of the average number of BrdU positive luminal epithelial and myoepithelial cells per organoid section. Proliferation in basal media (BM) was present only in luminal cells at a level of  $3 \pm 0.9$  BrdU positive cells per organoid section. R5020 treatment yielded  $4 \pm 0.4$  BrdU positive luminal cells per organoid section; no myoepithelial cell proliferation was seen. HGF increased proliferation only in luminal epithelial cells to a level of  $6 \pm 0.5$  BrdU positive cells per organoid section; no myoepithelial cell proliferation was seen. Proliferation in HGF+R5020-treated organoids increased the average BrdU positive luminal cells per organoid section to  $8 \pm 0.9$ . Interestingly, only HGF+R5020 treatment led to proliferation of myoepithelial cells. In HGF+R5020-treated organoids approximately  $2 \pm 0.5$  myoepithelial cells per organoid section were proliferating. These results demonstrate that the majority of proliferation occurred in the luminal cells and only the combination of HGF+R5020 was mitogenic for myoepithelial cells.

### ***In Vivo* Expression of c-Met Protein During Mouse Mammary Gland Development**

Expression of c-Met protein was examined in both epithelial sub-types of the mammary gland, luminal epithelial cells and myoepithelial cells, during different stages of mouse mammary gland development and in the different structures of the gland. The developmental stages of puberty (5wks), sexual maturity (10wks), mid-pregnancy, and seven days of lactation were examined to determine if the expression was developmentally regulated *in vivo*. Tissue sections were stained with an anti- c-Met antibody and an anti SMA antibody to detect myoepithelial cells. This allowed us to

differentiate the expression of c-Met in luminal epithelial cells vs. myoepithelial cells.

Images were captured using laser scanning confocal microscopy and were then analyzed by measuring the mean fluorescence intensity per cell of c-Met labeled cells.

Shown in Figure 9 is the quantitation of the expression of c-Met protein within luminal epithelial cells and myoepithelial cells at the different stages of the mouse mammary gland development. No differences in c-Met expression were observed in luminal epithelial cells at the different developmental stages. This was also true for the expression of c-Met for both ducts and alveoli. Therefore, the expression of c-Met within the luminal epithelial cells did not appear to be developmentally regulated.

In myoepithelial cells there was slightly lower expression of c-Met in pregnant and lactating ducts, but not in lobules, when compared to other stages. Otherwise, the expression of c-Met within the myoepithelial cells also did not appear to be developmentally regulated. However, in all structures and during all developmental stages it was found that the myoepithelial cells expressed c-Met at a higher level when compared to luminal epithelial cells.

### ***In Vitro* Expression of c-Met Protein in Response to Culture Treatments**

Expression of c-Met protein was examined in both luminal epithelial and myoepithelial cells in cultured organoids in response to the treatments with 1) BM, 2) HGF alone (50ng/ml), 3) R5020 (20nM), and 4) HGF + R5020 (50ng/ml + 20nM). Epithelial organoids plated in collagen gel cultures for 24, 48, and 72 hrs were prepared as sections. The sections were double labeled with c-Met and SMA. The DNA stain To-Pro 3-iodide was then used to stain the nuclei of all cells. Images were captured using

laser scanning confocal microscopy and analyzed by measuring the mean c-Met fluorescence intensity per cell.

Shown in Figure 10A is the quantitation of expression of c-Met within luminal epithelial cells expressed as fold increase over BM at the same time point. Fold increase of fluorescence intensity over BM was used for comparisons because different time points were obtained from separate experiments. No significant differences were observed among the different treatment groups at any of the time points examined. The expression of c-Met within the luminal epithelial cells did not appear to be altered by any of the treatments.

Shown in figure 10B is the quantitation of expression of c-Met within myoepithelial cells expressed as fold increase over BM at the same time point. No differences were observed among the different treatment groups at any of the time points examined. The expression of c-Met within the myoepithelial cells did not appear to be altered by any of the treatments.

Figure 10C shows the average expression level of c-Met in luminal epithelial cells versus the myoepithelial cells for all three time points. This figure shows that the myoepithelial cells expressed c-Met at a higher level when compared to luminal epithelial cells. Taken together the results obtained from the *in vivo* and *in vitro* studies showed that c-Met expression did not appear to be hormonally regulated and was not a mechanism by which R5020 is affecting organoid responses.

### ***In Vitro* Expression of Cyclin D1 Protein**

Since cyclin D1 (D1) is required for alveologenesis *in vivo* (30), antibody labeling experiments were performed to examine D1 expression in cultured organoids to

determine if D1 expression was also important in the alveolar-like response to HGF+R5020 treatment. The expression of D1 was examined in adult organoid cultures treated with BM, HGF, R5020, and HGF+R5020.

Expression of D1 in the adult cultures was increased slightly over basal levels by the addition of either HGF or R5020 alone. However, the intensity of staining was low and expression was localized predominately in the cytoplasm (Figure 11A). The combination of HGF+R5020 led to increased staining intensity and an increase in the nuclear localization of D1. Cyclin D1 expression in the HGF+R5020-treated organoids was predominately localized in the nucleus in nearly 40% of total cells (both D1 positive and negative cells) (Figure 11B). However, recent review of the images of the organoids showed very few myoepithelial cells present and that the organoids were rather small. This indicates that the cultures used to generate the images were likely over-digested and that these experiments should be repeated.

### ***In Vitro* PR Isoform Protein Expression**

Recent work in our laboratory has shown that there is differential expression of the PR A and B isoforms during mouse mammary gland development (23). Since the expression of PR B appears to be important during alveologenesis, the expression of the PR isoforms was examined in our culture system to determine their role in the alveolar-like response of organoids to HGF+R5020 treatment.

#### **PR A Protein Expression**

Progesterone receptor A protein expression was examined at time 0, directly after plating organoids into the collagen gels, and approximately  $29.2\% \pm 2.5\%$  of the cells were positive. Our lab has observed a similar percentage of PR A positive epithelial

cells *in vivo* at 17-20 weeks of age. This was the same age as the mice used to obtain the mammary organoids and indicated that the organoid isolation process did not appear to alter PR A expression (23). Progesterone receptor A protein expression was examined in three separate cultures at 48 hrs and 72 hrs: cc-1-20-04, cc1-26-04, cc1-18-05. As seen in figure 12 there appeared to be little overall difference in the percent of PR A positive cells among the different treatment groups at the 48hr time point (Figure 12A). The data indicate a trend of PR A down-regulation by HGF+R5020 treatment at 72 hrs in the three cultures tested to date (Figure12B). However, due to variability and a small sample size statistical analysis was not performed.

#### PR B Protein Expression

At time 0 no expression of PR B was seen. This is in agreement with the observations *in vivo* for the adult virgin (23). Progesterone receptor B expression was examined at 48 hrs and 72 hrs in two cultures: cc1-20-04 and cc1-26-04. Figure13 shows the expression of PR B was highest in both the 48 hr and 72 hr time points in organoids treated with HGF+R5020. These results indicate a trend of an increase of PR B positive cells at 48 and 72 hrs in response to HGF+R5020 treatment (Figure 13A&B).

From the results of the PR A and PR B protein expression studies it is clear that there is variability among the cultures. The variability may be due mainly to the lack of a sufficient number of samples. Therefore, additional experiments with these cultures should be done to obtain larger sample sizes to allow for statistical analysis.

#### **c-Met Signaling Pathway Inhibitor Studies**

In order to examine the roles of different signaling pathways in the response of mammary organoids to the culture treatments, studies using inhibitors of specific

signaling intermediates were used. Using this technique allowed for the targeting of specific pathways that are believed to be important for the proliferative and morphologic responses of mammary cells to HGF and R5020.

### PI3K Pathway

Previous studies in normal mammary epithelial and breast cancer cell lines have implicated the PI3K/AKT pathway in HGF-induced proliferation and tubulogenesis (51). Therefore, the effect of the PI3K inhibitor, LY294002, on the responses of primary culture organoids was examined. The PI3K inhibitor was initially tested at concentrations of 5, 10, and 20  $\mu\text{M}$ . The 5  $\mu\text{M}$  concentration was chosen since it resulted in the best viability of the organoids that was only slightly decreased vs. control-treated cultures.

### Effect of PI3K and AKT Inhibitors on Proliferation

In these experiments 17 $\beta$ -estradiol (E) was added since a further increase in proliferation was seen when E is added in addition to HGF+R5020 in our primary mammary organoids (64) and E is also known to induce expression of PR *in vivo* (65). DMSO-treated controls showed the same proliferative and morphologic responses as seen in controls without DMSO. Hepatocyte growth factor induced a 4-fold increase in proliferation over BM; HGF+R5020 yielded an 8-fold increase and HGF+E+R5020 a 13-fold increase at 72 hrs (Figure 14A). Inhibition of PI3K decreased proliferation by 25% in BM. Proliferation in HGF treated organoids was inhibited 57% in the presence of the PI3K inhibitor. Proliferation in HGF+R5020- and HGF+E+R5020-treated organoids were inhibited at 50% and 72% respectively, in the presence of the PI3K inhibitor (Figure 14B).



It has been shown that PI3K in addition to activating AKT can act as an adaptor protein at the c-Met receptor (41). In cultured rat oval cells, hepatic precursor cells, it was seen that inhibition of PI3K led to decreased ERK 1/2 activity (66). In order to investigate the possibility that the results obtained with the PI3K inhibitor were due to its effect on other pathways, an AKT inhibitor was also used. If similar responses were observed in organoids treated with an AKT inhibitor, it was likely that the effects of the PI3K inhibitor were specific to the PI3K/AKT pathway. It was observed that organoids treated with the AKT inhibitor showed a similar responses as the LY294002-treated organoids (Figure 14C). Proliferation was decreased by 55% in HGF-treated organoids and by 42% in HGF+R5020 treated organoids (Figure 14D). This suggests that the effects of the PI3K inhibitor were specific to the PI3K/AKT pathway.

#### Effect of PI3K and AKT Inhibitors on Cell Type Specific Morphology of Mammary Organoids

Visual inspection of LY294002-treated organoids showed minor decreases in tubule length and number. Using the *in situ* collagen gel antibody staining protocol, SMA staining was severely diminished in all treatment groups at 72 hrs in LY294002-treated organoids (Figure 15). To investigate the possibility that the results of PI3K inhibitor were due to its effect on other pathways, an AKT inhibitor was also used. It was observed that organoids treated with the AKT inhibitor showed the same response as the PI3K inhibitor treated organoids. Smooth muscle actin staining was severely diminished in all treatment groups at 72 hrs (Figure 16).

In the absence of SMA expressing cells the luminal cells were still able to form tubules. However, cellular extensions and chains of cells did not appear to be present. A

time course experiment was then performed in order to examine when the loss of SMA expression occurred. Hepatocyte growth factor-treated organoids were labeled at 24, 48, and 72 hrs for actin and SMA in the presence of 5 $\mu$ M LY. As seen in figure 17, SMA expression was present at 24 hrs, diminished at 48 hrs, and severely diminished at 72 hrs.

From the PI3K time course experiment it was not possible to determine if the loss of SMA expression was due to increased sensitivity of the myoepithelial cells to cytotoxic effects of the PI3K inhibitor. Experiments in which the PI3K inhibitor was washed out after 24 hrs of treatment were performed to address this question. If the effects of the PI3K inhibitor were the result of a permanent change in the organoids, LY294002-treated organoids should not express SMA at 72hr after the inhibitor was washed out. If the effects were reversible and dependent on the continued presence of LY294002 in the culture media, then LY294002-treated organoids should show expression of SMA at 72 hrs after the inhibitor was washed out. It was observed that the expression of SMA was rescued by 72 hrs if the inhibitor was washed out of the media at 24 hrs (Figure 17). This suggests that the loss of SMA expression was not due to increased cytotoxicity of the inhibitor to the myoepithelial cells, but rather to inhibition of SMA protein expression.

#### ERK Pathway

Studies in mammary tissues have also implicated a role for the ERK1/2 pathway in HGF-induced proliferation (51). The MEK 1/2 inhibitor, U0126, which inhibits both MEK 1 and 2 equally, was used to determine the importance of the ERK 1/2 pathway in the response of the culture organoids. The effects of U0126 were tested at a 10 $\mu$ M concentration. This concentration was chosen based upon previous studies in other

culture systems (46) and upon minimal effect on cell viability based on our own cell viability results.

#### Effect of MEK 1/2 Inhibitor on Proliferation

Dimethyl sulfoxide-treated controls exhibited the same proliferative and morphological responses as non-treated controls at 72 hrs (Figure 18A). Proliferation in U0126-treated organoids in BM was decreased 45%. Cultures treated with HGF, HGF+R5020, or HGF+E+R5020 all showed similar decreases in proliferation of about 55% (Figure 18B).

#### Effect of MEK 1/2 Inhibitor on Cell Type Specific Morphology of Mammary Organoids

While no quantitative data was obtained on the morphology (tubule number and length) of the U0126 treated cultures, visual inspection showed minor decreases in tubule length and number. As seen in figure 19, myoepithelial cells in organoids treated with BM+U0126 exhibited normal morphology. This was also true of R5020-treated organoids. In HGF- or HGF+R5020- treated organoids the myoepithelial cells were no longer elongated but instead were rounded up and were present throughout the organoids. Luminal cells did not appear to be altered morphologically under inhibitor treatment. Luminal epithelial cells were present in the main body of the organoids and were able to form cellular extensions and tubules; unlike the myoepithelial cells, the luminal cells did not appear rounded. These results suggest that the ERK 1/2 pathway is important in both the proliferative response of the luminal epithelial cells and the morphological response of myoepithelial cells in response to treatment with HGF or HGF+R5020.

### Matrix Metalloproteinase Inhibition

Matrix metalloproteinases appear to have a role in the development of the mammary gland *in vivo* (57), and in tubulogenesis in primary mouse mammary organoids (60). Therefore, we investigated the role of MMPs in mammary organoids by treating organoids with a MMP inhibitor and determining the effect on proliferation and morphology. A broad spectrum MMP inhibitor, GM6001, was used at a 10 $\mu$ M concentration. The concentration was chosen based upon its use in a organoid culture system similar to ours (60).

### Effect of MMP Inhibitor on Proliferation

Dimethyl sulfoxide treated organoids exhibited a typical response with a strong HGF proliferative response similar to control cultures without DMSO. Hepatocyte growth factor+R5020-induced proliferation was increased over that of HGF alone (Figure 20A). Proliferation in organoids treated with BM in the presence of GM6001 was decreased 50%. Hepatocyte growth factor- and HGF+R5020-treated organoids showed a decrease in proliferation of 74% when treated with GM6001 (Figure 20B).

### Effect of MMP Inhibitor on Cell Type Specific Morphology of Mammary Organoids

*In situ* labeling of the organoids showed that inhibition of MMPs did not appear to have an affect on the morphology of myoepithelial cells (Figure 21). However, morphology of HGF- and HGF+R5020-treated organoids was altered in response GM6001 treatment. In the control treated counterparts the tubulogenic morphology was mostly comprised of cords and tubules of cells, while the organoids treated with GM6001 appeared to have only cellular extensions and chains of cells. These results suggest that activity of MMPs were necessary for proliferation of luminal cells in the organoids and

were also needed for the formation of cords and tubules in response to HGF or HGF+R5020 treatment.

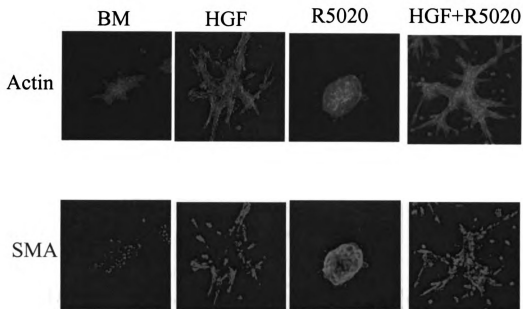


Figure 6 . Luminal epithelial and myoepithelial cell morphologies in response to culture treatments. Images are a projection images constructed from a z-series captured on a confocal microscope. Organoids were treated with BM, HGF, R5020, and HGF+R5020. Green images are stained with phalloidin conjugated with Alexa-488 which stained actin, and labeled all cells. Red images are stained for smooth muscle actin (SMA), which is a specific marker of myoepithelial cells. Note the elongated myoepithelial cells in the HGF- and HGF+R5020-treated organoids and the cyst of luminal cells surrounded by myoepithelial cells in the R5020-treated organoid (mag. 200X).

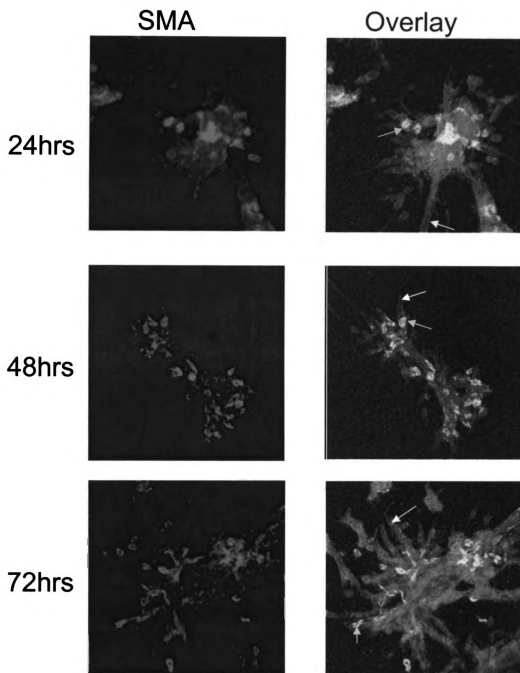


Figure 7. Time course of luminal and myoepithelial cell morphology in HGF-treated organoids. Images are projection images constructed from a z-series captured on a confocal microscope. Red images are stained for smooth muscle actin (SMA), which is a specific marker of myoepithelial cells. Overlay image is the combination of SMA staining and the staining of organoids with phalloidin conjugated with Alexa-488, which stained actin, and labeled all cells. White arrows indicate cellular extensions of luminal cells. Yellow arrows indicate myoepithelial cells in extensions. Note that luminal epithelial cells and not myoepithelial cells were at the leading edge of extensions. (mag. 200x).

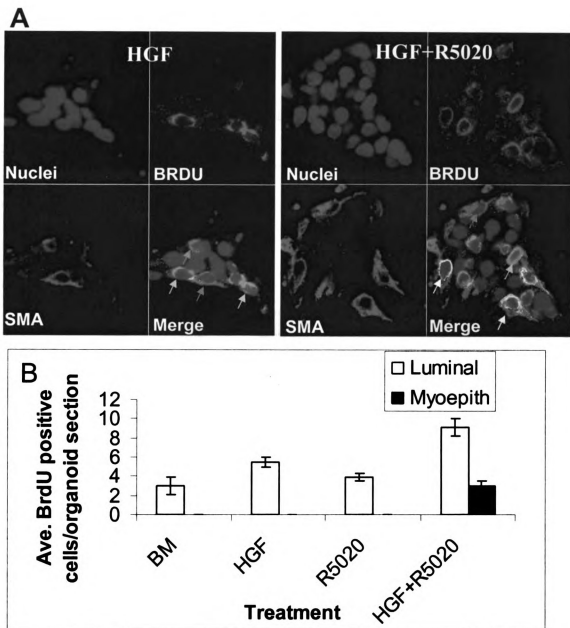


Figure 8. Cell type specific proliferation at 72hrs. A. Representative staining of HGF and HGF+R5020 treated organoids. Blue staining represents cell nuclei. Green staining represents BrdU positive cells. Red staining cells are positive for the myoepithelial marker, smooth muscle actin (SMA). The merge image is a composite of the three other images. White arrows indicate proliferating myoepithelial cells, which are only present in HGF+R5020 treated organoids. Yellow arrows indicate proliferating luminal cells and blue arrows indicate myoepithelial cells that are not proliferating. (mag. 400x) B. Quantitation of average BrdU positive cells per organoid section. White bars indicate the mean number of luminal epithelial cells proliferating per organoid section  $\pm$  SEM. Black bars indicate the mean number of myoepithelial cells proliferating per organoid section  $\pm$  SEM.



### **c-Met Expression in Luminal vs. Myoepithelial Cells in vivo**

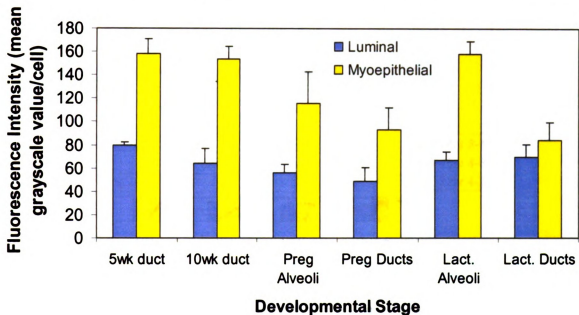


Figure 9. Analysis of expression of c-Met during the mammary gland developmental stages of puberty (5wks), sexual maturity (10wks), pregnancy (ducts and alveoli), and lactation (ducts and alveoli). Comparison of c-Met expression in luminal epithelial vs. myoepithelial cells. Each bar= mean  $\pm$  S.E.M.

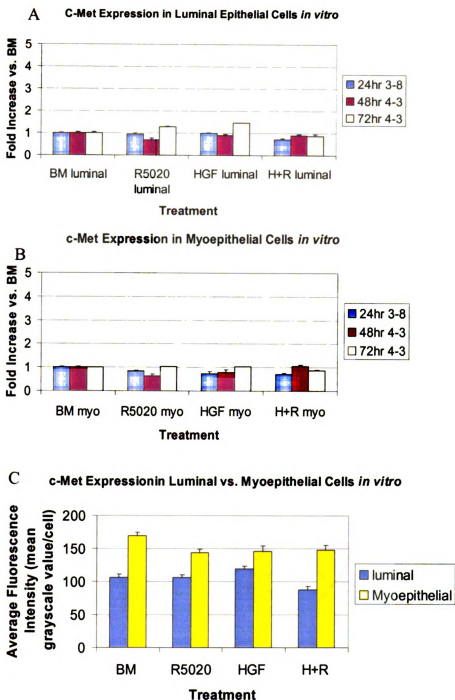


Figure 10. Effect of culture treatments on c-Met protein expression in epithelial organoids cultured in collagen gels. Mammary epithelial cells in collagen gels were cultured alone (BM), in R5020 (10nM), in HGF (50ng/ml), or in HGF (50ng/ml) + R5020 (10nM) (H+R). A. Expression of c-Met within luminal epithelial cells, B. Expression of c-Met within myoepithelial cells. C. Expression of c-Met in luminal epithelial cells vs. myoepithelial cells. Each bar = mean  $\pm$  S.E.M.

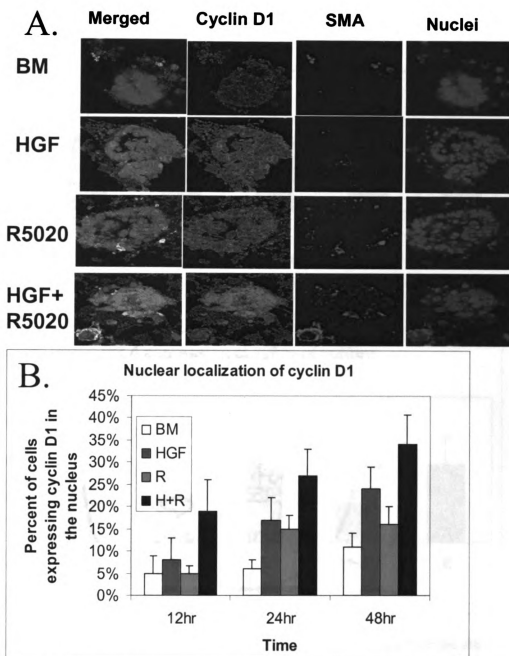


Figure 11. Cyclin D1 expression in adult cultured organoids A. Representative images showing D1 expression in adult cultured organoids. Green images represent D1 expression, red images represent myoepithelial cells, and blue images represent the nuclei of all cells in the organoid. The merged image is an overlay of the three separate images. (mag. 630x) B. Nuclear localization of Cyclin D1. Percentage of cells expressing cyclin D1 localized in the nucleus under treatments of BM, HGF, R5020 (R), and HGF+R5020 (H+R) Each bar= mean  $\pm$  range (n=2).

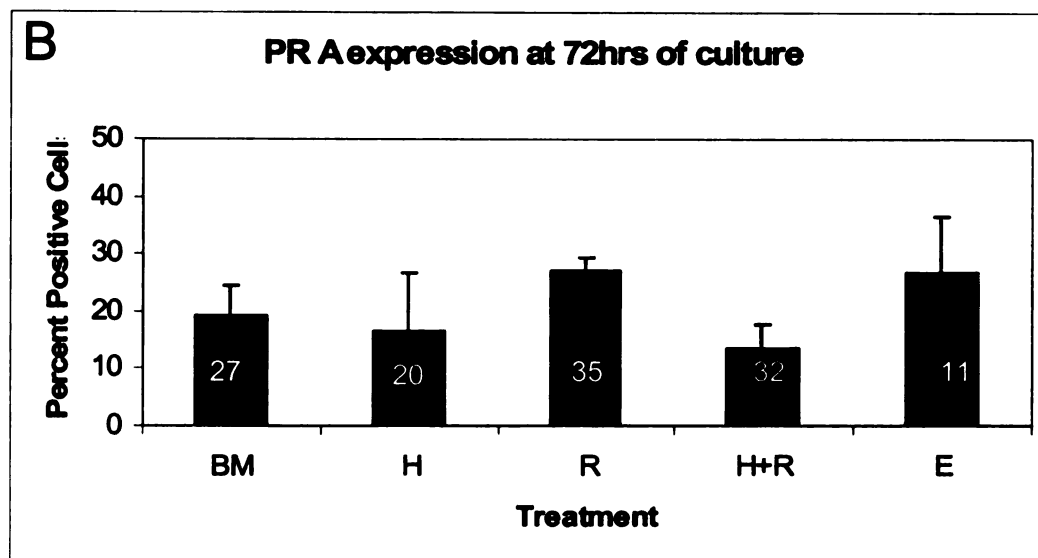
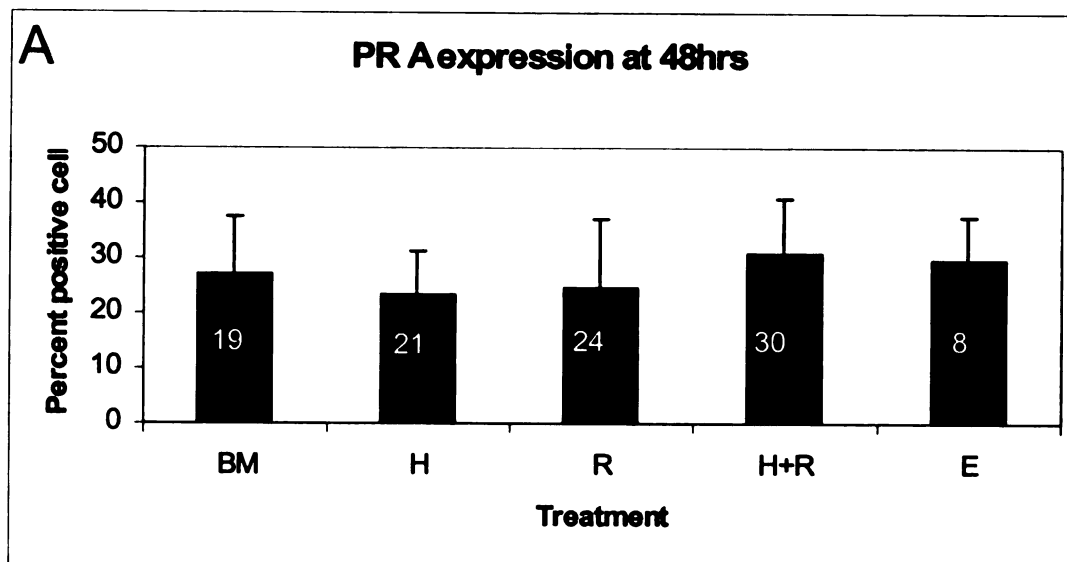


Figure 12. PRA expression in cultured organoids. The results presented are averages of three different cultures (cc1-20-04, cc1-26-04, and cc1-18-05). A. PR A expression at 48hrs. Percentage of total cells positive for PR A at time points of 48hrs. B. PR A expression at 72hrs. Percentage of total cells positive for PR A at time points 72hrs. Organoids were treated with BM, HGF (H), R5020 (R), HGF+R5020 (H+R), and estrogen (E). Each bar=mean  $\pm$  SEM. Number in bars indicates the total number of organoids sampled from all cultures. Due to sample size and variability no statistical analysis was performed.

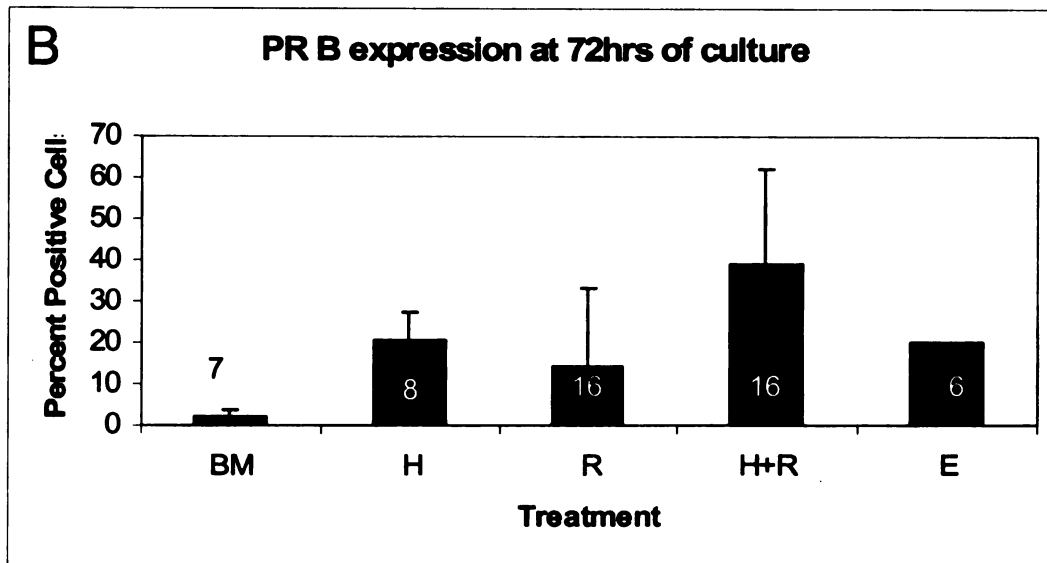
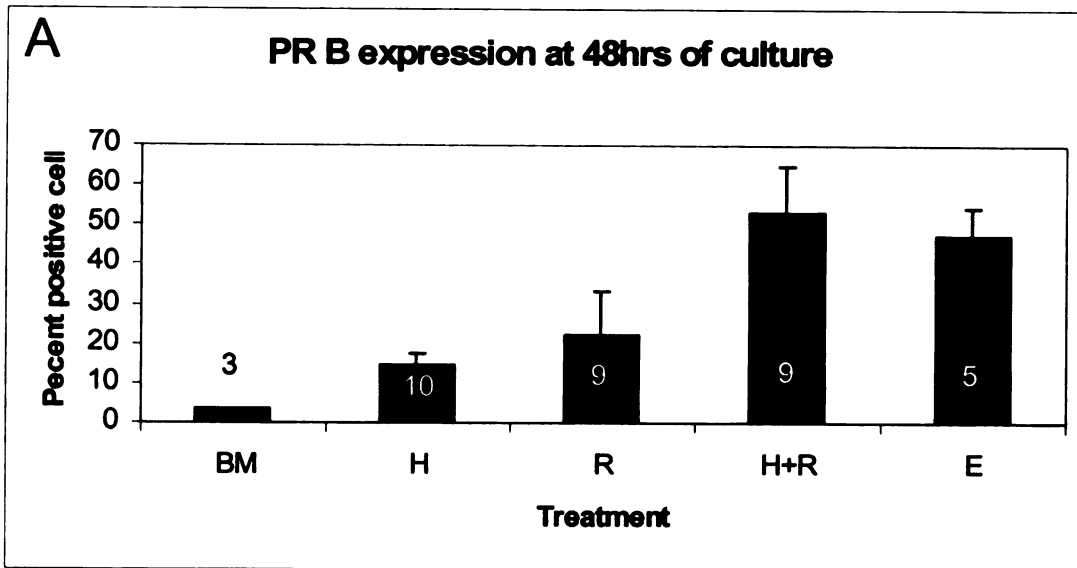
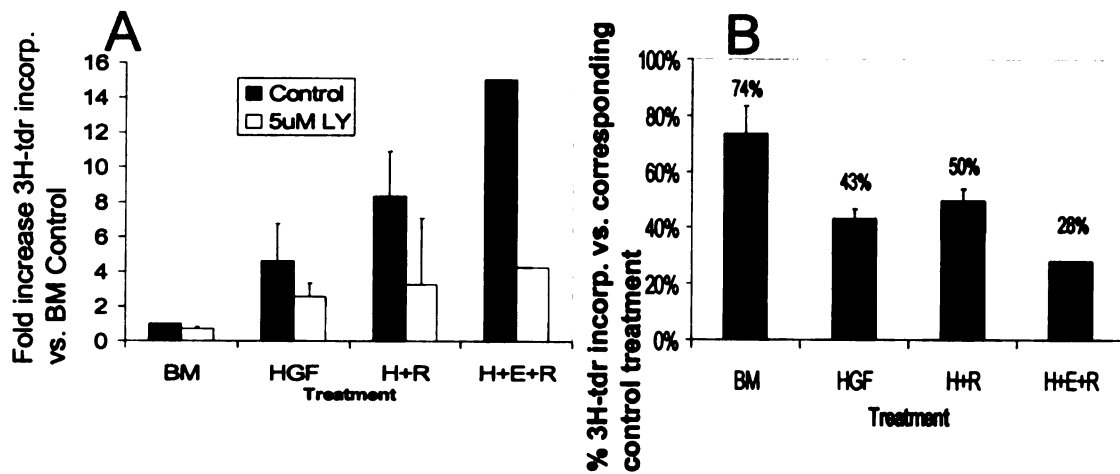


Figure 13. PRB expression in cultured organoids. The results presented are the average of two separate cultures (cc1-20-04 and cc1-26-04). A. PR B expression at 48hrs. Percentage of total cells positive for PR A at time points of 48hrs. B. PR B expression at 72hrs. Percentage of total cells positive for PR B at time points 72hrs. Organoids were treated with BM, HGF (H), R5020 (R), HGF+R5020 (H+R), and estrogen (E). Each bar=mean  $\pm$  standard deviation. Number in bars indicates the total number of organoids sampled from all cultures. Due to sample size and variability no statistical analysis was performed.

### Effect of PI3K inhibition at 72hrs



### Effect of AKT inhibition at 72hrs

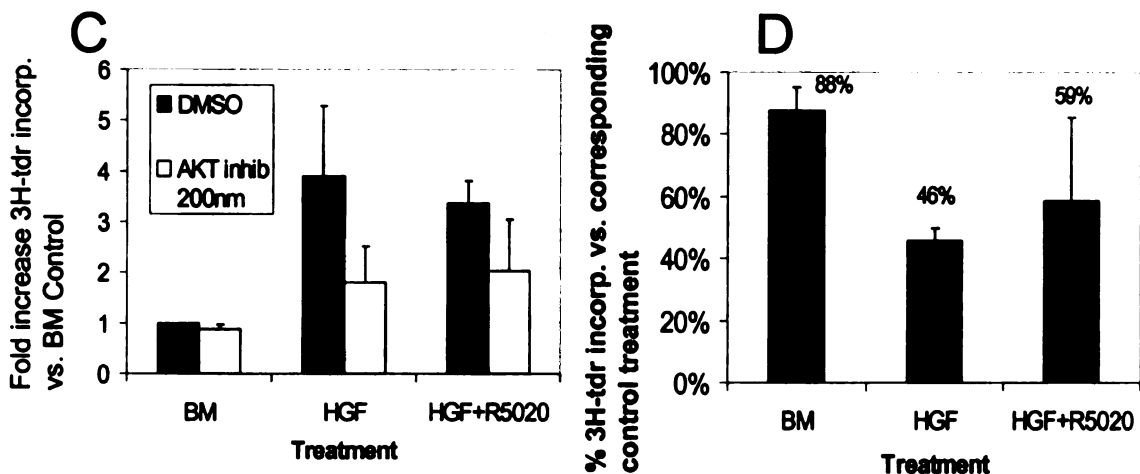


Figure 14. Effects of PI3K and AKT inhibition on HGF- and R5020-dependent proliferation at 72hrs. A. Effect of PI3K inhibition. Fold increase in proliferation measured by  $^3\text{H}$ -thymidine incorporation was calculated versus BM of control treatments under an inhibitor concentration of  $5\mu\text{M}$  LY294002. B. Effect of PI3K inhibition.  $^3\text{H}$ -tdr incorporation as a percentage of corresponding control treatment. C. Effect of AKT inhibition. Fold increase in proliferation measured by  $^3\text{H}$ -tdr incorporation was calculated versus BM of control treatments under an inhibitor concentration of  $200\text{ nM}$  AKT inhibitor IV. D. Effect of AKT inhibition.  $^3\text{H}$ -thymidine incorporation as a percentage of corresponding control treatment. Each bar = mean  $\pm$  SEM

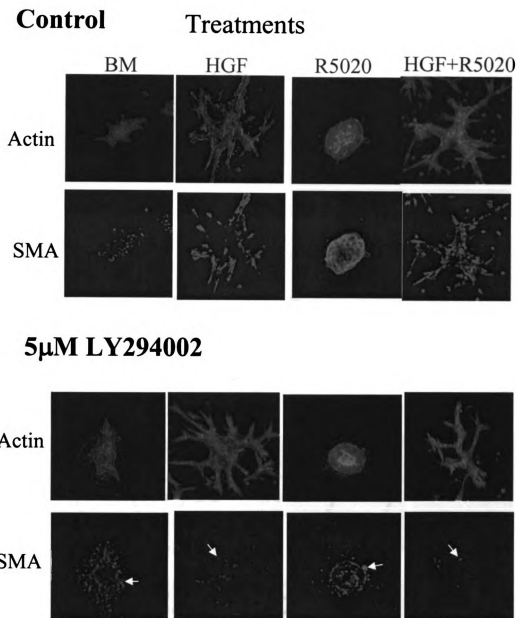


Figure 15. PI3K inhibitor effects on organoid, luminal, and myoepithelial cell morphologies. Images are a projection images constructed from a z-series captured on a confocal microscope. Organoids were treated as indicated. Green images were stained with phalloidin conjugated with Alexa-488, which stained actin, and labeled all cells. Red images are stained for smooth muscle actin (SMA), which is a specific marker of myoepithelial cells. Note the reduction of SMA expressing cells in LY294002-treated cultures, especially in HGF and HGF+R5020 treatments. White arrows indicate the reduction of SMA labeling (mag. 200x).

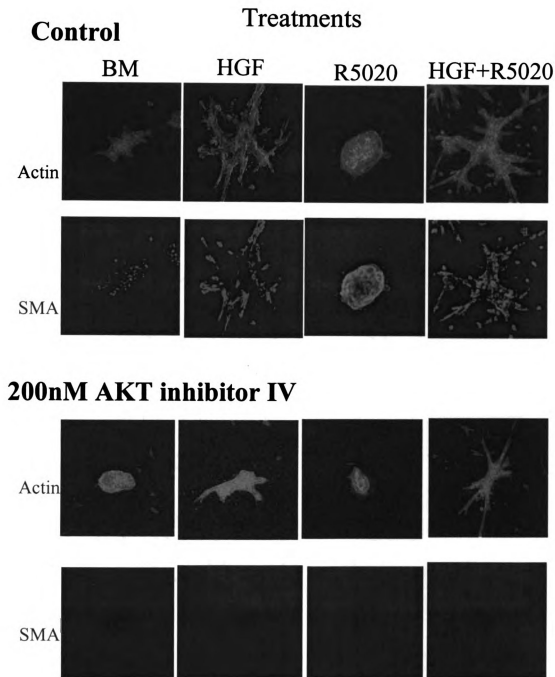


Figure 16. AKT inhibitor effects on organoid, luminal and myoepithelial cell morphologies. Images are a projection images constructed from a z-series captured on a confocal microscope. Organoids were treated as indicated. Green images were stained with phalloidin conjugated with Alexa-488, which stained actin, and labeled all cells. Red images are stained for smooth muscle actin (SMA), which is a specific marker of myoepithelial cells. Note the absence of SMA expressing cells in AKT inhibitor IV-treated organoids (mag. 200x).



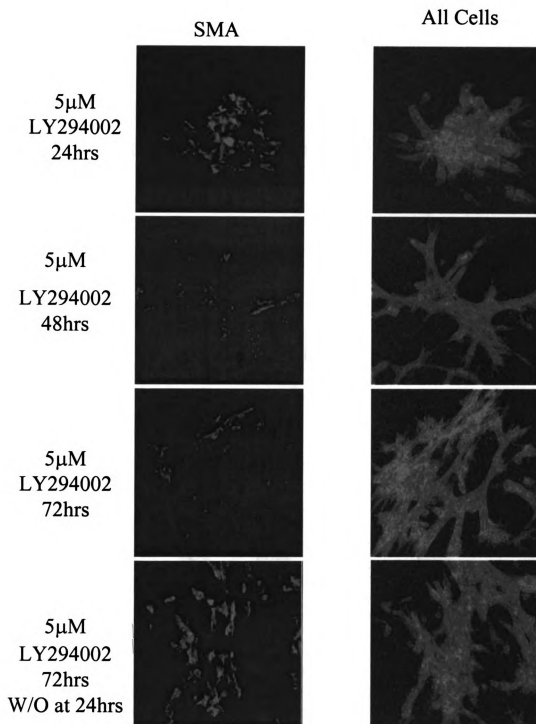


Figure 17 . Time course of luminal and myoepithelial cell morphology in HGF-treated organoids in the presence of 5 $\mu$ M LY. Images are a projection images constructed from a z-series captured on a confocal microscope. Red images are stained for smooth muscle actin (SMA), which is a specific marker of myoepithelial cells. Green image is the staining of organoids with phalloidin conjugated with Alexa-488, which stained actin, and labeled all cells. Note that SMA expressing cells are present at 24hrs of LY294002 treatment and are lost by 72hrs. Wash-out of PI3K inhibitor at 24hrs resulted in the rescue of SMA expressing cells at 72hrs. (mag. 200x)

## Effect of MEK1/2 inhibition at 72hrs

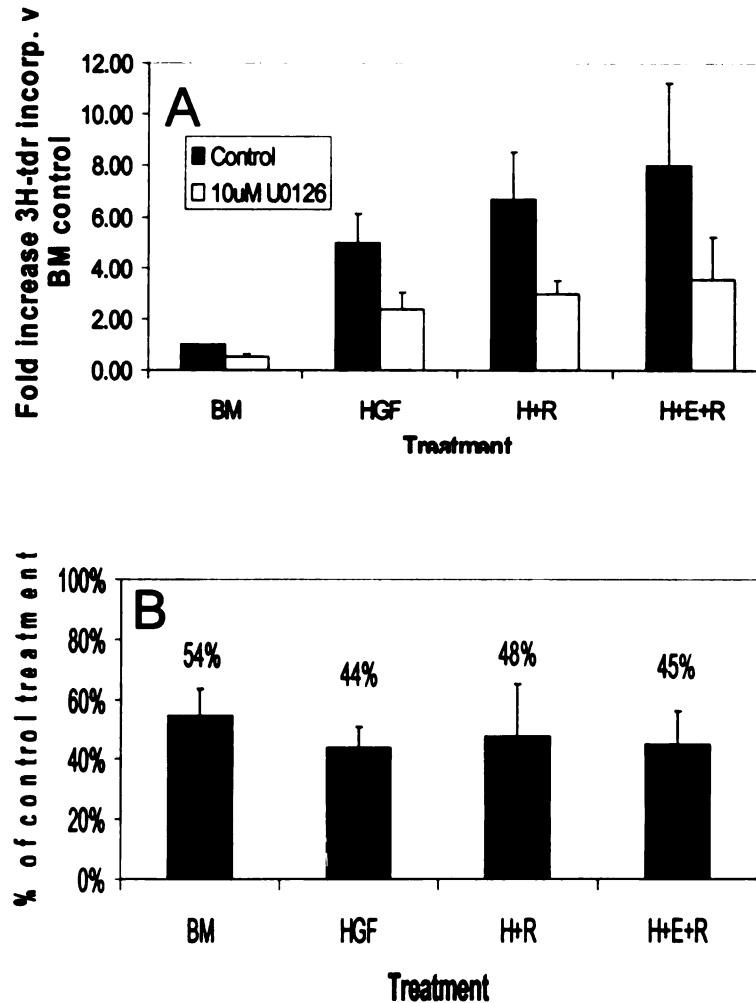
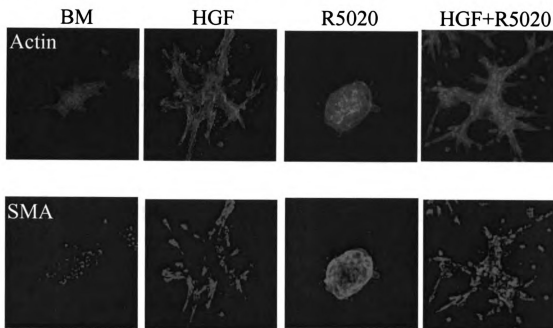


Figure 18. A. Effect of MEK 1/2 inhibition on proliferation at 72hrs. A. Fold increase in proliferation determined by 3H-tdr incorporation was calculated versus BM of control treatments. A concentration of 10 $\mu$ M U0126 was used. B. Effect of MEK1/2 inhibition. Percentage of 3H-tdr incorporation as a percentage of corresponding control treatment. Each bar = mean  $\pm$  SEM

## Control

## Treatments



## 10 $\mu$ M U0126

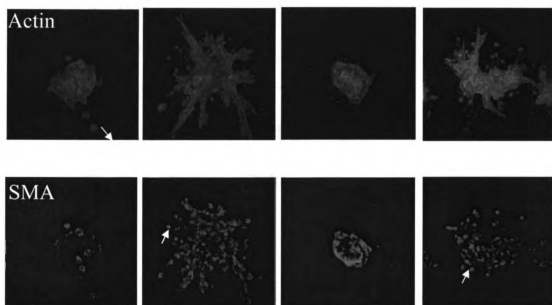


Figure 19. MEK 1/2 inhibitor effects on organoid, luminal and myoepithelial cell morphologies. Images are a projection images constructed from a z-series captured on a confocal scope. Organoids were treated as indicated. Green images are stained with phalloidin conjugated with Alexa-488, which stained actin, and labeled all cells. Red images are stained for SMA, which is a specific marker of myoepithelial cells. Note the rounded morphology of the myoepithelial cells in U0126-treated organoids as indicated by the white arrows. (mag. 200x).

## Effect of MMP inhibition at 72hrs

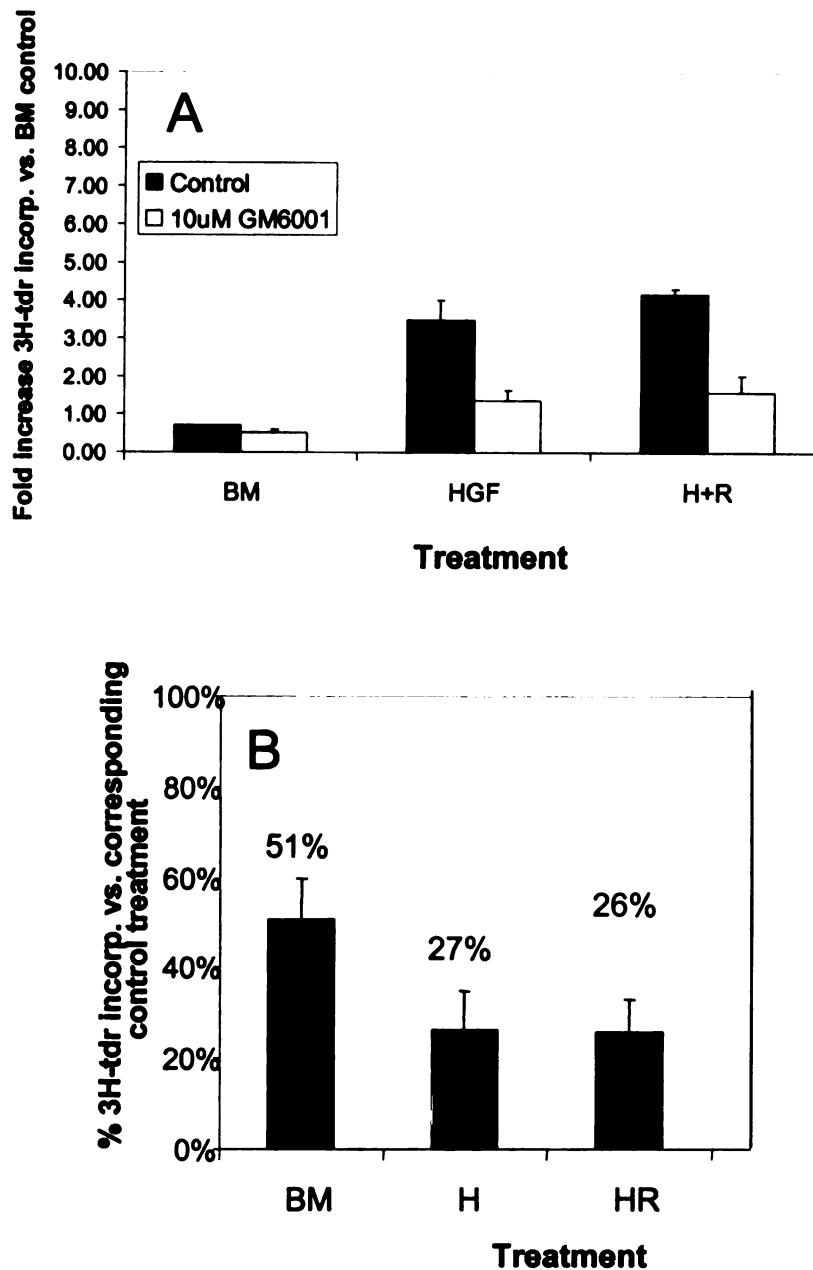


Figure 20. Effect of MMP inhibition on proliferation at 72hrs. A. Fold increase in proliferation determined by 3H-tdr incorporation was calculated versus BM of control treatments. An inhibitor concentration of 10 $\mu$ M GM6001 was used. B. Effect of MMP inhibition. 3H-tdr incorporation was expressed as a percentage of corresponding control treatment. Each bar = mean  $\pm$  SEM

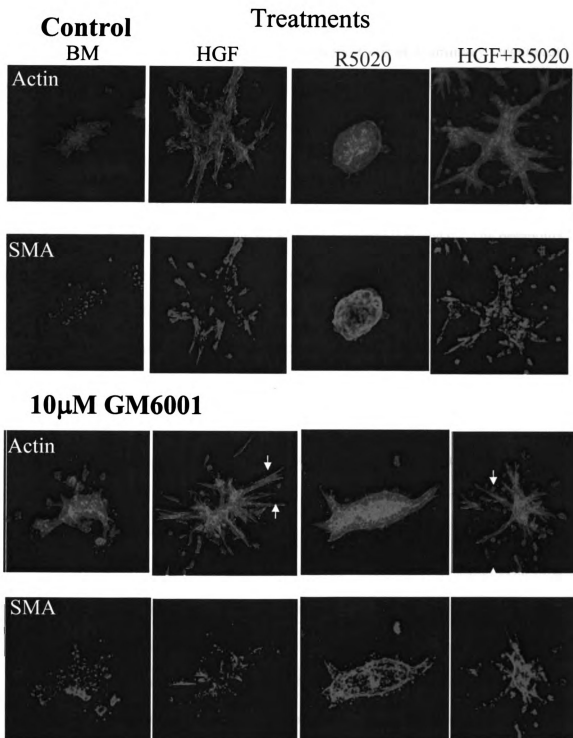


Figure 21. MMP inhibitor effects on organoid, luminal epithelial cell, and myoepithelial cell morphologies. Images are a projection images constructed from a z-series captured on a confocal microscope. Organoids were treated as indicated. Green images are stained with phalloidin conjugated with Alexa-488, which stained actin, and labeled all cells. Red images are stained for smooth muscle actin (SMA), which is a specific marker of myoepithelial cells. Note the presence only of extensions and chains of cells; cords and tubules are not present in GM6001-treated organoids. White arrows indicate chains and extensions. (mag. 200x).

## **Discussion**

### **The Roles of Luminal Epithelial and Myoepithelial Cells in Mammary Organoids**

#### **Morphology**

Previous work in our mammary organoid system has resulted in interesting observations of organoid responses to HGF and HGF+R5020. Hepatocyte growth factor treatment of organoids leads to a tubulogenic morphology at 72 hrs, while organoids treated with HGF+R5020 results in an alveolar-like morphology (64). The organoids consist of both luminal epithelial and myoepithelial cells. This is important because our model system more closely resembles the gland architecture *in vivo*, and therefore we can gain a better understanding of how both types of mammary epithelial cells respond to defined stimuli. Previously what role the two epithelial subtypes play in the organoid responses to the various culture treatments has not been defined.

To address this question we adapted an *in situ* antibody labeling technique used in MDCK cells in order to examine both the location and morphology of luminal epithelial and myoepithelial cells in the organoids. Organoids treated with BM showed both luminal and myoepithelial cells organized as a group with the myoepithelial cells external to the luminal cells. In response to HGF treatment at 72 hrs the myoepithelial cells were elongated and were present mainly in tubules branching off the organoids. Luminal cells were present both in tubules and in the main body of organoids. R5020 treatment resulted in the myoepithelial cells localized external to and surrounding luminal cells that had formed cyst-like structures. Hepatocyte growth factor+R5020 treatment resulted in elongated myoepithelial cells in the tubules, and more myoepithelial cells were present in the main body of the organoids. The luminal cells were present both in the tubules and in

the main organoid body. These results demonstrate that morphology change in our organoids is due to changes occurring in both luminal epithelial and myoepithelial cells.

Observations of HGF- and HGF+R5020-treated organoids suggest that the myoepithelial cells play an important role in the formation of the tubules, since most tubules contained elongated myoepithelial cells by 72 hrs, the time of maximal tubule formation. While the role of myoepithelial cells in tubule formation is not known, results from the time course study suggest that myoepithelial cells were not responsible for initiating the extensions that form tubules. Smooth muscle actin labeling at 24 and 48 hrs showed that while the myoepithelial cells were present in the chains of cells, the leading edge of most extensions were not SMA expressing cells but were most likely luminal epithelial cells. This would suggest that luminal cells lead the extension stage in tubule formation and myoepithelial cells migrate in behind to continue the tubule formation that creates the tubulogenic morphology in our culture system. The observation that the luminal cells formed the initial cellular extensions conflicts earlier published work on separated human luminal epithelial and myoepithelial cells. It was previously seen that purified luminal cells do not respond morphologically to HGF (39). In our system this was not true. However, it is possible that the ability of luminal epithelial cells to respond morphologically to HGF requires the presence of myoepithelial cells.

Two models of tubulogenesis in response to HGF have been generated in MDCK cells. The first model suggests that tubules form from cellular extensions, which progress into chains of cells, followed by the formation of cords, and finally tubules. Tubules formed in this model do not have a continuous lumen throughout the formation of the tubule, but rather have a discontinuous lumen which is connected to the main lumen by

the migration of cells once cords are formed (45). The second model suggests that a continuous lumen is always present and that tubules are the result of basal protrusions of two or more cells together, with a lumen present between them (47). However, both of these models were generated in a MDCK cell line system. The MDCK cell line is a homogeneous epithelial cell line. This is quite different from our organoid system which has a heterogeneous cell population containing both luminal epithelial and myoepithelial cells. This latter organization more closely resembles the mammary gland *in vivo*. It appears from images captured from the in situ labeling assay that tubulogenesis in our system is similar to the four-step model of tubule formation. Both cellular extension and chains of cells were present in our in situ labeling which would seem to rule out continuous lumen model. To our knowledge, our study is the first to examine the roles of both mammary luminal epithelial and myoepithelial cells together in the formation of tubules and alveolar-like structures.

Since myoepithelial cells do not express either isoform of PR (10) the myoepithelial staining pattern in R5020-treated organoids, myoepithelial cells surrounding a cyst of luminal cells, suggests that R5020 acted on the luminal cells through PR to produce a paracrine factor that in turn acted on the myoepithelial cells. This was apparent in both R5020- and HGF+R5020-treated organoids. Myoepithelial cells in both treatments had altered morphology when compared to either BM- or HGF-treated organoids. The identity of this factor is not known, but studies performed by others offer a potential candidate. Wnt-4 is a secreted protein that is synthesized in luminal epithelial cells which express PR and has been shown to be up-regulated by P (29). Wnt-4 is also important *in vivo* for the side-branching that takes place during early-



mid pregnancy (29). These findings support the idea that Wnt-4 could be acting on myoepithelial cells in our system to alter organoid morphology in response to R5020 and to increase the numbers of myoepithelial cells in HGF+R5020-treated organoids.

### **Cell Type Specific Proliferation**

While proliferation assays, such as incorporation of tritiated-thymidine ( $^3\text{H}$ -tdr) assays, can provide important insights to proliferation of cells in different systems, they have a major drawback. In systems with heterogeneous cell populations, such as our mammary organoid culture system, the  $^3\text{H}$ -tdr assay can only address overall changes in proliferation among treatments. It cannot examine changes in proliferation in specific cell types when they are grown together. Since our culture organoids are composed of both luminal and myoepithelial cells, we felt it was important to examine the proliferative responses to treatments in both cell types. This was accomplished using immunohistochemical staining of organoids with BrdU, a thymidine base analog, combined with staining for the myoepithelial cell marker SMA. This allowed for quantitation of proliferating luminal vs. myoepithelial cells. While the majority of the proliferation occurred in the luminal cells under both HGF and HGF+R5020 treatment, it was only under HGF+R5020 treatment that proliferation also occurred in the myoepithelial cells. This indicates that at least a portion of the synergistic increase in proliferation seen in response to HGF+R5020 treatment could be attributed to increased myoepithelial cell proliferation and that both HGF+R5020 are required.

However, since myoepithelial cells do not express PR, the mechanism by which the myoepithelial cells are stimulated to proliferate is most likely through a paracrine mechanism. Wnt-4 is again a likely target. Recent work in our lab addressed a similar

question *in vivo*. Ovariectomized adult mice were injected with saline (control), E, or E+P. The E+P response in the mammary gland *in vivo* is similar to our HGF+R5020 response *in vitro* in that both result in increased proliferation and an alveolar-like morphology. It was also observed that only in mice treated with E+P that proliferation was strongly stimulated in myoepithelial cells (personal communication with Mr. Aupperlee). Overall, it appears that cell type specific proliferation of mammary myoepithelial cells may play an important role in preparing the mammary gland for pregnancy since their proliferation is only stimulated under alveologenic stimuli, such as E+P treatment.

### **c-Met Protein Expression**

Since HGF is required for the proliferative and morphological responses to R5020, this directed us to analyze how R5020 may affect c-Met activated signaling pathways that mediate proliferation and tubulogenesis. One logical target to investigate was c-Met itself. Since progestins act through the PR, the possibility existed that R5020, through the PR, could act to alter c-Met protein levels through transcriptional regulation. In order to address this question c-Met protein levels were examined in the organoid culture system.

### **In Vivo Studies**

Results from our developmental study of c-Met protein expression showed that expression levels of c-Met were not significantly different at puberty, sexual maturity, pregnancy or lactation. Our results also showed higher c-Met expression in myoepithelial cells compared to luminal epithelial cells. To our knowledge this is the

first study that has examined c-Met protein expression within the specific epithelial subtypes of the mammary gland.

### *In Vitro* Studies

Our experiments also examined the protein expression levels of c-Met in our *in vitro* culture system in organoids treated with BM, HGF, R5020, and HGF+R5020. c-Met expression was not significantly different among the treatment groups at any of the time points tested in either luminal or myoepithelial cells. Again, higher levels of c-Met expression were seen in myoepithelial cells when compared to luminal epithelial cells.

Overall from the *in vivo* and *in vitro* studies a number of conclusions were reached. First, the protein expression of c-Met does not appear to be developmentally or hormonally regulated as evidenced by the similarity of expression levels among developmental stages *in vivo* and hormone treatment groups *in vitro*. Second, the protein expression of c-Met is higher in the myoepithelial cells than in the luminal epithelial cells. This difference is observed both *in vivo* and *in vitro*. Third, the protein expression levels of c-Met as measured by fluorescence intensity within the different cell types were similar *in vivo* and *in vitro*. This finding indicates that with respect to c-Met protein expression our culture model system reflects the behavior of these two cell types *in vivo*. Finally, since no differences in c-Met expression were observed under treatment with and without R5020, it is unlikely that the alveolar-like response seen in HGF+R5020-treated organoids is due to changes in c-Met expression.

Previous studies that examined development expression of c-Met mRNA *in vivo* have left some confusion due to their conflicting nature. One study using a Northern blot assay shows that c-Met mRNA expression is first seen during puberty at around 5 weeks

of age in the mouse. Maximal expression then occurs at 12 weeks of age, which was the oldest age of nulliparous mice tested. Expression of c-Met is then lost in late pregnancy and lactation (39). In this same study the mRNA levels of separated primary human luminal and myoepithelial cells exhibited higher c-Met mRNA expression in the luminal cells vs. the myoepithelial cells (39). A second study using an RNase protection assay in mouse mammary glands shows c-Met mRNA expression increasing through puberty and no down-regulation of c-Met during late pregnancy or lactation (40). All these previous c-Met expression studies were done using mRNA from homogenized glandular tissue and did not address developmental regulation of c-Met protein expression. Therefore, little is known about the relative developmental expression of the c-Met protein in the luminal vs. myoepithelial cells of the mammary gland. Our results are in agreement with the study which observed no down-regulation of the c-Met message during pregnancy or lactation in the mouse mammary gland (40). When viewed in the light of both our *in vitro* results and our *in vivo* results the lack of regulation during development seems logical. If the c-Met mRNA was down-regulated during pregnancy it would seem to indicate that c-Met would be regulated by progestins, which we did not observe *in vitro*. Our results on the expression of the c-Met receptor protein in luminal epithelial vs. myoepithelial cells conflict with the study that examined c-Met mRNA expression in these two cell types. Our experiments cannot answer this discrepancy; however, since the previous study, which was carried out in human cells, examined only mRNA expression, it is possible that the mechanism of regulation may be different in human cells or may not be at the transcriptional level, but instead may be translational regulation or differential turnover of c-Met.

## Cyclin D1

Cyclin D1 has many important actions that it performs in the nucleus, such as phosphorylation of the retinoblastoma protein and the titration of p27<sup>Kip1</sup> (67). Cyclin D1 is expressed throughout the cell cycle but is located in the nucleus during the G<sub>1</sub> phase of the cell cycle, and is then redistributed to the cytoplasm during S phase (67). In our system we observed that HGF, R5020, and HGF+R5020 treatment of organoids increased the expression of cyclin D1 protein when compared to BM. However, it was only in HGF+R5020-treated organoids that 45% of the total cells showed nuclear localization of cyclin D1. Nuclear localization of the cyclin D1 protein is important in allowing cells to pass through the G<sub>1</sub>-S checkpoint of the cell cycle (67). Since nuclear localization was correlated with increased proliferation in our system, these results seem to indicate that the increased nuclear localization of cyclin D1 was needed for the synergistic increase in proliferation seen in response to HGF+R5020 treatment.

The increase seen in cyclin D1 expression in HGF and R5020-treated organoids is in agreement with other studies that showed that both HGF and P can lead to increased cyclin D1 expression. Hepatocyte growth factor has been shown to increase transcription of cyclin D1 mRNA by microarray analysis in human glioblastoma cells (68). *In vivo*, P has been shown to increase both transcriptional and protein expression of cyclin D1 in the mouse mammary gland (69). To our knowledge this study is the first to examine the effects of combined HGF+R5020 treatment on cyclin D1 expression. Our results indicate that increased expression of cyclin D1 and its localization to the nucleus may be important factors in mediating the HGF+R5020 response seen in the mammary organoids cultures. It appears that the expression of D1 at high levels in the nucleus may be

important for increased proliferation to occur in response to HGF+R5020 treatment in this system. However, re-analysis of the cultures used for the cyclin D1 protein expression studies showed a relative absence of myoepithelial cells by SMA labeling. Loss of SMA staining in the sectioned organoids likely indicates that the cultures used in these experiments were over-digested. Since it is not possible to determine if over-digestion could have altered the staining pattern of cyclin D1, further studies on other cultures will be needed to confirm what has been observed in the present studies.

### **PR Isoform Protein Expression**

Progesterone is a potent mitogen in the mammary gland. It has an especially important role in the development of the mammary gland during pregnancy. The spatio-temporal expression pattern of the PR A and B isoforms observed *in vivo* has increased our understanding of when and where the two isoforms may be acting in the mouse mammary gland (23). Progesterone receptor A protein expression is present in the virgin mammary gland as early as 3 weeks of age in luminal epithelial cells. The number of PR A positive cells, nearly 50%, does not change much through puberty and is at similar levels in the sexually mature mouse. As the nulliparous mice age further, the number of PR A positive cells decreases to near 30% in mouse mammary glands at 17-20 weeks of age. The number of PR A positive cells then decreases dramatically during pregnancy; only 10% of luminal epithelial cells express PR A at 14 days of pregnancy. Progesterone receptor B is expressed only during pregnancy with almost half of all luminal cells positive for PR B at 14 days of pregnancy, suggesting that expression of PR B is important in alveologenesis.

We believe that the mouse mammary organoid responses, increased proliferation and alveolar-like morphology, represent an *in vitro* model of events seen in early pregnancy. To further characterize the culture system, we examined the protein expression of the PR A and PR B isoforms. The results showed that PR A expression decreased in HGF+R5020-treated organoids while PR B expression increased in the same organoids. This suggests that PR protein expression in our model system also reflects PR protein expression *in vivo* under alveologenic conditions.

Previously, our lab has shown that that HGF expression can be upregulated *in vitro* by E treatment of mammary fibroblasts (70). The *in vivo* studies on PR isoform expression suggest that PR isoform expression is at least partially mediated by steroid hormones. It is possible that *in vivo*, HGF protein expression could be induced by the high levels of E present at pregnancy and could then interact with P in the mammary epithelial cells to bring about the changes seen during pregnancy. Only E is present at high levels in the pubertal and adult mouse and it is only during pregnancy that both E and P are present at high levels. It would therefore seem possible that the E+P response seen *in vivo* may additionally be caused by the interaction of HGF and P.

The results showing a decrease in PR A and an increase in PR B in response to HGF+R5020 treatment suggest that the increased proliferation and alveolar-like morphology are most likely mediated through PR B. *In vivo* studies in the PR B K/O mouse as well as PR B over-expressing transgenic mice *in vivo* support this hypothesis. Mammary glands in the PRB K/O mice are unable to form alveoli in response to pregnancy (26). Over-expression of PR B results in the precocious formation of alveoli in the mammary glands of virgin mice (71).

While this study gives some insight into the role of the PR isoforms in the response seen to HGF+R5020, many other directions could be followed in order to further investigate the roles of the PR isoforms in our organoids culture system. The phosphorylation status of the PR isoforms in response to HGF+R5020 treatment could be examined, since phosphorylation of PR by pathways induced by growth factors is believed to be important in synergistically increasing expression of PR regulated genes (72). This could be accomplished by either western blot or by immunohistochemical staining of organoids for the phosphorylated form of PR. The mechanism of PR isoform regulation could also be examined in the culture system as well. From the present studies, PR isoform expression is altered to a lesser extent compared to what is observed *in vivo*. *In vivo* it is only during alveologenesis at pregnancy that PR B is expressed. However, we observed that in the organoids treated only with BM that PR B expression was seen as early as 24 hrs. Since no PR B expression is observed in organoids at time 0, this indicates that some type of regulation, possibly suppressing PR B protein expression present *in vivo* is lost when the organoids are placed into collagen culture.

Again, from the results of both the PR A and PR B protein expression studies it is clear that there is variability among the cultures. Therefore, additional experiments should be done to obtain larger sample sizes in order to confirm the trends that were observed.

### **Inhibitor Treatment of Cultures**

The c-Met receptor has multi-substrate docking sites in its intracellular portion, to which adaptor and other signaling molecules that interact with the receptor must bind (41). Due to this, mutants at these docking sites affect a large number of signaling



cascades, which makes it difficult to determine what functions different signaling cascades perform in response to HGF (41). One way to determine the roles of different signaling pathways is through the use of chemical inhibitors to downstream signaling intermediates. While some inhibitors may affect multiple signaling molecules, most of the inhibitors available today are quite specific if used at the proper concentration. Therefore, in order to determine the roles of different signaling cascades in mediating the response of mammary organoids to the culture treatments we used inhibitors targeted to downstream signaling intermediates of pathways that are activated in response to HGF.

### PI3K/AKT

Previous studies in normal human mammary epithelial cell lines as well as in other cell types such as rat oval cells (66) have implicated the PI3K/AKT pathway in HGF-induced proliferation and tubulogenesis (51). Therefore, inhibitors of this pathway were used in order to examine the roles of PI3K and AKT in our organoid culture system. In PI3K- and AKT inhibitor-treated cultures the proliferation and morphology of the organoids was altered at 72 hrs of culture. The inhibitors reduced both HGF- and HGF+R5020-dependent proliferation. A similar decrease in proliferation was seen in HGF-treated rat oval cells in the presence of the PI3K inhibitor (66).

The PI3K and AKT inhibitors also led to the loss of SMA expression in the organoids, which could have been due to the loss of myoepithelial cells. There are a number of hypotheses that may explain the decrease in proliferation and/or the loss of SMA staining. First, PI3K inhibition may be more cytotoxic to myoepithelial cells than luminal cells at the 5 $\mu$ M concentration used; this would explain the loss of SMA expression and the subsequent death of the myoepithelial cells may have contributed to

the proliferation decrease seen in the HGF+R5020 treatment. A study involving washout of the inhibitor at 24 hrs was done to address this question. If the inhibitor was truly cytotoxic to the myoepithelial cells, then treatment with the inhibitor would likely kill many of the myoepithelial cells by 24 hrs. If expression of SMA was able to return after washing out the inhibitor, it would suggest that the inhibitor was having an effect on the expression of the SMA protein. It was observed that the expression of SMA returned to control levels by 72 hrs if the inhibitor was washed out of the media at 24 hrs. This indicated that the loss of SMA expression was not due to increased cytotoxicity of the inhibitor to the myoepithelial cells. Viability staining of the organoids also suggests that increased cytotoxicity is not the case since all inhibitors were seen to cause cell death, at levels only slightly higher than the control organoids.

Second, the inhibition of PI3K may block differentiation of precursor cells present in the organoids. This hypothesis could explain the loss of SMA expression in our organoids but not the loss of proliferation. A time course study was done using the *in situ* antibody labeling to help provide an answer. If fewer myoepithelial cells were observed at time zero or at time points earlier than 72 hrs it would suggest that precursor cells may be differentiating to form the organoids observed at 72 hrs; if similar numbers are observed at time 0 and 72 hrs it would suggest that the myoepithelial cells are more sensitive to the PI3K inhibitor. While quantitation was not done, general inspection of the organoids showed that similar numbers of SMA expressing cells were present at 24 through 72 hrs in the control treated organoids. This would indicate that the loss of SMA expressing cells was not due to the inhibitor causing failure of precursor cells to differentiate into myoepithelial cells.

Finally, inhibition of PI3K signaling may block the expression of the SMA protein. While this can explain the loss of SMA staining it does not explain the decrease in luminal epithelial cell proliferation caused by the inhibitor. The time course and inhibitor washout studies suggest that inhibition of SMA protein expression is the most likely explanation for the loss of SMA expression in organoids treated with inhibitors of PI3K or AKT.

In the absence of SMA expressing cells the luminal epithelial cells were still able to form tubules in response to HGF and HGF+R5020. The major effect seen on the luminal cells under inhibition of either pathway was a decrease in proliferation. Both PI3K and AKT inhibition led to decreases in proliferation. We speculate that the decrease in proliferation could be due to the loss of inhibition on glycogen synthase kinase-3 $\beta$  (GSK-3 $\beta$ ), whose activity is down-regulated by active AKT (67). Glycogen synthase kinase-3 $\beta$  has been shown to be a negative regulator of cyclin D1 expression in NIH-3T3 cells (67). Inhibition of AKT in our system may have increased the activity of GSK-3 $\beta$  which in turn may have down-regulated cyclin D1 expression levels, and led to a decrease in proliferation. Although the specific mechanism remains to be identified, it appears that the PI3K/AKT pathway is necessary for HGF and HGF+R5020 induced proliferation in luminal cells.

Overall, the PI3K or AKT inhibitors appeared to have the same effects on both proliferation and morphology, which suggests that the effects are specific to the PI3K/AKT pathway. Also both inhibitors appeared to have their greatest effect on myoepithelial cells. Both inhibitors blocked the expression of SMA. Organoids treated with either inhibitor exhibited fewer tubules that were also decreased in length. A study

in MDCK cells has shown that PI3K is activated in response to HGF and is upstream of the Rho family kinases, which are involved in actin polymerization and therefore are important in motility and morphological responses (73). The presence of PI3K activity has also been shown to be required for the down-regulation of E-cadherin in response to HGF which will also promote cell motility and morphology responses such as cellular extensions (74). Therefore, it is likely that the PI3K/AKT pathway is important in the morphology changes seen in the myoepithelial cells and to a lesser extent the luminal epithelial cells in response to the various treatments

Additional studies could be carried out in order to further elucidate the role of PI3K and AKT in the responses of our culture organoids. The expression of the cyclin D1 protein could be examined in the PI3K or AKT inhibitor-treated organoids to determine what role PI3K and AKT are playing in the induction of cyclin D1 expression in our system.

### ERK 1/2

Studies in normal human mammary cell lines have also implicated a role for the ERK1/2 pathway in HGF-induced proliferation (51). Recent studies in MDCK cells also suggests that the ERK 1/2 activity is needed for the first steps of HGF-induced tubule formation (46). Therefore, an inhibitor of this pathway (U0126) was used in order to examine ERK 1/2's role in our organoid culture system. Proliferation in U0126 treated organoids was decreased in the treatments of BM, HGF, HGF+R5020, and HGF+E+R5020, which all showed similar decreases in proliferation of about 50%.

Organoids also exhibited fewer tubules that were shorter under U0126 treatment. This did not appear to be the result of changes in SMA expression, as it was not affected.

However, the overall morphology of SMA expressing cells was affected. The cells were not elongated as seen in the controls under HGF or HGF+R5020 treatments, but were instead rounded up. The rounded shape may explain loss of the ability of myoepithelial cells to form extensions and chains when ERK 1/2 signaling is blocked (46). Luminal cells appeared to have a normal morphology.

Activity of ERK 1/2 in MDCK cells has been shown to be important in the formation of cellular extensions (37, 46). High level of protein expression of activated ERK 1/2 has been shown to be sufficient to induce cellular extension in the absence of any growth factors but must be down-regulated in order for tubules to form (75). It was also shown in MDCK cells that when ERK 1/2 signaling is blocked in response to U0126, cysts of MDCK cell are unable to make cellular extensions and chains of cells in response to HGF treatment (46). In our system the myoepithelial cells may play a role in chain formation because elongated myoepithelial cells are found in most chains and tubules, and this ability may be partially blocked by U0126 treatment. It is possible that inhibition of ERK 1/2 in our system is not allowing the cells to alter their shape. However, luminal epithelial cells in our system appear to maintain their ability to form extensions and chains of cell in the presence of U0126. Therefore it appears that the myoepithelial cells are more sensitive to ERK 1/2 inhibition than luminal epithelial cells or that different pathways are activated in the two epithelial cell types.

The inhibition of proliferation seen in the presence of the ERK pathway inhibitor would seem to indicate that the ERK 1/2 pathway has a role in mediating HGF-induced proliferation, and due to the increased loss of proliferation in the BM-treated organoids it would also seem that some ERK activity is needed to maintain the basal levels of

proliferation in the organoids. Studies in human lens epithelial cells have shown that HGF-induced proliferation and induction of cyclin D1 are dependent on the activity of ERK 1/2 (76). Since changes were present in both the myoepithelial cell morphology and in proliferation in our study, ERK1/2 signaling was an important mediator of both luminal and myoepithelial responses to HGF and HGF+R5020.

Additional studies could be carried out in order to further elucidate the role of ERK1/2 in the responses of our culture organoids. A time course study using the in situ labeling method could be used to examine when the myoepithelial cells become rounded. Expression of the cyclin D1 protein could also be examined in the U0126-treated organoids to determine what role ERK 1/2 is playing in the induction of cyclin D1 expression in each cell type. Since the ERK 1/2 pathway is known to phosphorylate PR and increase its transcriptional activity (77), the phosphorylation status of both PR isoforms could be examined in the presence or absence of the MEK1/2 inhibitor to determine if the phosphorylation of the PR by the ERK 1/2 pathway is important in the organoid system responses.

### Matrix Metalloproteinases

The broad spectrum MMP inhibitor used in our experiments caused the greatest decrease in HGF and HGF+R5020-dependent proliferation and had the least effect on the morphology of the myoepithelial cells within organoids. This indicates that the MMP inhibitor likely had the greatest effect on the luminal epithelial cells. One possible hypothesis is MMPs may be needed in order for the luminal cells to alter the surrounding matrix to allow for proliferation and movement of luminal epithelial cells into the collagen matrix. Without MMPs present, the luminal cells may be unable to spread out

and proliferation may be blocked due to contact inhibition. It may also be that MMPs are needed to clip certain membrane proteins such as E-cadherin which contribute to the activation of proliferation signaling pathways (59). A model had been proposed in which MMP 3 cleaves the E-cadherin complex and releases free  $\beta$ -catenin into the cytoplasm where it then translocates to the nucleus. Once in the nucleus,  $\beta$ -catenin can act as a transcription factor and induce increased expression of a number of proliferation inducing proteins, such as cyclin D1(59).

While our results do provide some insight about the role of MMPs in our culture system, they also provide many avenues for future research. It would be of interest to learn which cells are producing the MMPs in our system and if MMPs are being regulated differently under the various treatments. Previous studies in primary rat mammary epithelial organoids suggest that both the luminal and myoepithelial cells are capable of producing MMPs. The rat mammary epithelial organoids were seen to produce both MMP-2 and MMP-9, and both MMP-2 and MMP-9 expression were up-regulated by treatment with P (61). Treatment of mouse mammary epithelial organoids with HGF has also been shown to increase expression of MMP-2 and MMP-3 (60). Since the MMP inhibitor had such a profound effect on HGF- and HGF+R5020-induced proliferation it is likely that HGF and HGF+R5020 are capable of inducing MMP expression in our system. The regulation of MMP expression could be examined through microarray or real time polymerase chain reaction analysis of the different treatment groups. Treatment of the cultures with inhibitors specific for MMP2 or MMP3 could also be used in order to determine what roles they may have in our system in relation to their different roles in the development of the mammary gland *in vivo* (57). The

expression of the cyclin D1 protein could also be examined in the GM6001-treated organoids to determine if MMPs are altering expression of cyclin D1 in the organoids.

The use of signaling intermediate inhibitors to examine pathways in response to HGF and HGF+R5020 has allowed us to examine the roles of the PI3K/AKT, ERK 1/2, and MMPs. The PI3K/AKT and ERK1/2 pathways were chosen because both are major HGF signaling intermediates in most systems that show a response to HGF. Matrix metalloproteinases have been shown to be secreted in response to P in rat mammary epithelial cells and in response to HGF in mouse primary mammary epithelial cells (60, 61) and have major roles in normal mammary gland development (57). However, these pathways are not the only possible targets that our organoid system may be using to achieve the responses seen.

Additional signaling intermediates could be examined to further elucidate what pathways our organoids system uses in both proliferation and in morphology change. The SH2-domain-containing inositol 5-phosphatase (SHIP) proteins 1 and 2 have been shown to be involved in tubulogenic responses of MDCK cells to HGF as shown by both overexpression and mutant studies (53). Both SHIP 1 and 2 are capable of binding directly to c-Met and when over-expressed lead to increased formation of lamellipodium (53).

$\beta$ -catenin is known to be involved in both the wnt signaling pathways as well as downstream of c-Met (78).  $\beta$ -catenin is likely important for the morphologic and proliferative responses of our organoids.  $\beta$ -catenin is part of adhesion complexes along with E-cadherin and  $\alpha$ -catenin. Hepatocyte growth factor can cause the dissociation of  $\beta$ -catenin from these complexes and allow it to translocate to the nucleus where it can



function as a transcription factor (78). One of the genes that is up-regulated in response to  $\beta$ -catenin is D1 (78). Thus it is possible that  $\beta$ -catenin may also have an important role in the organoid responses seen in our system.

Src has been shown to interact directly with the c-Met protein and to be important in proliferation and motility of the mouse mammary cancer cell line, SP1 (79). Many of these other pathways are likely important in the organoid responses in our system and could be studied.

## **Summary**

In conclusion, our organoid system has allowed us to generate a number of interesting results that show the importance of studying both epithelial subtypes of the mammary gland together. Only in HGF+R5020-treated organoids was a proliferative response seen in myoepithelial cells. *In situ* antibody labeling together with investigation of cell type specific proliferation indicate that a paracrine factor was likely released from PR positive luminal cells in response to R5020 that can alter both proliferation and morphology of PR negative myoepithelial cells. c-Met protein expression was examined in luminal epithelial and myoepithelial cells both *in vivo* and *in vitro* and it was found that changes in c-Met protein expression was not a mechanism by which R5020 affected the HGF-induced increase in proliferation or altered morphology. Nuclear expression of cyclin D1 and PR B in luminal cells was correlated with increased proliferation and alveolar-like morphology in the organoids.

Studies of inhibitors of PI3K/AKT, ERK1/2, and MMPs showed different effects on luminal epithelial and myoepithelial cells. Activity of PI3K and AKT were found to be important in maintaining expression of SMA in myoepithelial cells, and inhibition of

either intermediate led to decreased proliferation in the luminal epithelial cells.

Inhibition of the ERK 1/2 pathway affected myoepithelial cell morphology causing them to round up; also proliferation was decreased in luminal cells. Matrix metalloproteinase inhibition greatly decreased proliferation of luminal epithelial cells, while it seemed to have very little effect on myoepithelial cells. Overall, these results provide the basis for further studies to determine the mechanism by which P acts alone and with HGF within the mammary gland to bring about proliferation and morphology change. These studies show the importance of using *in vitro* model systems that closely mirror cellular organizations present *in vivo*.

## References

1. **Hofseth LJ, Raafat AM, Osuch JR, Pathak DR, Slomski CA, Haslam SZ** 1999 Hormone replacement therapy with estrogen or estrogen plus medroxyprogesterone acetate is associated with increased epithelial proliferation in the normal postmenopausal breast. *Journal of Clinical Endocrinology & Metabolism* 84:4559-65
2. **Magnusson C, Persson I, Adami HO** 2000 More about: effect of hormone replacement therapy on breast cancer risk: estrogen versus estrogen plus progestin. *J Natl Cancer Inst* 92:1183-4.
3. **Ross RK, Paganini-Hill A, Wan PC, Pike MC** 2000 Effect of hormone replacement therapy on breast cancer risk: estrogen versus estrogen plus progestin. *J Natl Cancer Inst* 92:328-32.
4. **Schairer C, Lubin J, Troisi R, Sturgeon S, Brinton L, Hoover R** 2000 Menopausal estrogen and estrogen-progestin replacement therapy and breast cancer risk. *Jama* 283:485-91.
5. 2002 Risks and benefits of estrogen plus progestin in healthy postmenopausal women. *JAMA* 288:321-333
6. **Fendrick JL, Raafat AM, Haslam SZ** 1998 Mammary gland growth and development from the postnatal period to postmenopause: ovarian steroid receptor ontogeny and regulation in the mouse. *J Mammary Gland Biol Neoplasia* 3:7-22.
7. **Woodward TL, Xie JW, Haslam SZ** 1998 The role of mammary stroma in modulating the proliferative response to ovarian hormones in the normal mammary gland. *Journal of Mammary Gland Biology & Neoplasia* 3:117-31
8. **Deugnier MA, Teuliere J, Faraldo MM, Thiery JP, Glukhova MA** 2002 The importance of being a myoepithelial cell. *Breast Cancer Res* 4:224-30
9. **Barsky SH** 2003 Myoepithelial mRNA expression profiling reveals a common tumor-suppressor phenotype. *Exp Mol Pathol* 74:113-22
10. **Shyamala G, Barcellos-Hoff MH, Toft D, Yang X** 1997 In situ localization of progesterone receptors in normal mouse mammary glands: absence of receptors in the connective and adipose stroma and a heterogeneous distribution in the epithelium. *J Steroid Biochem Mol Biol* 63:251-9.

11. **Shao ZM, Radziszewski WJ, Barsky SH** 2000 Tamoxifen enhances myoepithelial cell suppression of human breast carcinoma progression in vitro by two different effector mechanisms. *Cancer Lett* 157:133-44
12. **Couse JF, Korach KS** 1999 Estrogen receptor null mice: what have we learned and where will they lead us? *Endocr Rev* 20:358-417
13. **Briskin C, Park S, Vass T, Lydon JP, O'Malley BW, Weinberg RA** 1998 A paracrine role for the epithelial progesterone receptor in mammary gland development. *Proc Natl Acad Sci U S A* 95:5076-81.
14. **Gudjonsson T, Ronnov-Jessen L, Villadsen R, Rank F, Bissell MJ, Petersen OW** 2002 Normal and tumor-derived myoepithelial cells differ in their ability to interact with luminal breast epithelial cells for polarity and basement membrane deposition. *J Cell Sci* 115:39-50
15. **Sternlicht MD, Kedeshian P, Shao ZM, Safarians S, Barsky SH** 1997 The human myoepithelial cell is a natural tumor suppressor. *Clin Cancer Res* 3:1949-58
16. **Miller C, Pavlova A, Sassoon DA** 1998 Differential expression patterns of Wnt genes in the murine female reproductive tract during development and the estrous cycle. *Mech Dev* 76:91-9
17. **Humphreys RC, Lydon J, O'Malley BW, Rosen JM** 1997 Mammary gland development is mediated by both stromal and epithelial progesterone receptors. *Mol Endocrinol* 11:801-11
18. **Lydon JP, Sivaraman L, Conneely OM** 2000 A reappraisal of progesterone action in the mammary gland. *J Mammary Gland Biol Neoplasia* 5:325-338
19. **Giangrande PH, McDonnell DP, Tetel MJ, Leonhardt SA, Edwards DP, Pollio G** 1999 The A and B isoforms of the human progesterone receptor: two functionally different transcription factors encoded by a single gene. *Recent Prog Horm Res* 54:291-313; discussion 313-4.
20. **Kastner P, Krust A, Turcotte B, Stropp U, Tora L, Gronemeyer H, Chambon P** 1990 Two distinct estrogen-regulated promoters generate transcripts encoding the two functionally different human progesterone receptor forms A and B. *Embo J* 9:1603-14
21. **Hovland AR, Powell RL, Takimoto GS, Tung L, Horwitz KB** 1998 An N-terminal inhibitory function, IF, suppresses transcription by the A-isoform but not the B-isoform of human progesterone receptors. *J Biol Chem* 273:5455-60.

22. **Richer JK, Jacobsen BM, Manning NG, Abel MG, Wolf DM, Horwitz KB** 2002 Differential gene regulation by the two progesterone receptor isoforms in human breast cancer cells. *J Biol Chem* 277:5209-18.
23. **Aupperlee MD, Smith KT, Kariagina A, Haslam SZ** 2005 Progesterone receptor isoforms A and B: temporal and spatial differences in expression during murine mammary gland development. *Endocrinology* 146:3577-88
24. **Qiu M, Lange CA** 2003 MAP kinases couple multiple functions of human progesterone receptors: degradation, transcriptional synergy, and nuclear association. *J Steroid Biochem Mol Biol* 85:147-57.
25. **Boonyaratanakornkit V, Scott MP, Ribon V, Sherman L, Anderson SM, Maller JL, Miller WT, Edwards DP** 2001 Progesterone receptor contains a proline-rich motif that directly interacts with SH3 domains and activates c-Src family tyrosine kinases. *Mol Cell* 8:269-80.
26. **Mulac-Jericevic B, Mullinax RA, DeMayo FJ, Lydon JP, Conneely OM** 2000 Subgroup of reproductive functions of progesterone mediated by progesterone receptor-B isoform. *Science* 289:1751-4.
27. **Mulac-Jericevic B, Lydon JP, DeMayo FJ, Conneely OM** 2003 Defective mammary gland morphogenesis in mice lacking the progesterone receptor B isoform. *Proc Natl Acad Sci U S A* 100:9744-9
28. **Dale TC** 1998 Signal transduction by the Wnt family of ligands. *Biochem J* 329 ( Pt 2):209-23
29. **Briskin C, Heineman A, Chavarria T, Elenbaas B, Tan J, Dey SK, McMahon JA, McMahon AP, Weinberg RA** 2000 Essential function of Wnt-4 in mammary gland development downstream of progesterone signaling. *Genes Dev* 14:650-4.
30. **Sicinski P, Weinberg RA** 1997 A specific role for cyclin D1 in mammary gland development. *J Mammary Gland Biol Neoplasia* 2:335-42
31. **Wulf GM, Ryo A, Wulf GG, Lee SW, Niu T, Petkova V, Lu KP** 2001 Pin1 is overexpressed in breast cancer and cooperates with Ras signaling in increasing the transcriptional activity of c-Jun towards cyclin D1. *Embo J* 20:3459-72
32. **Hsu W, Shakya R, Costantini F** 2001 Impaired mammary gland and lymphoid development caused by inducible expression of Axin in transgenic mice. *J Cell Biol* 155:1055-64
33. **Arteaga CL** 2004 Cdk inhibitor p27Kip1 and hormone dependence in breast cancer. *Clin Cancer Res* 10:368S-71S

34. **Robinson GW, Johnson PF, Hennighausen L, Sterneck E** 1998 The C/EBP $\beta$  transcription factor regulates epithelial cell proliferation and differentiation in the mammary gland. *Genes Dev* 12:1907-16
35. **Miyoshi K, Shillingford JM, Smith GH, Grimm SL, Wagner KU, Oka T, Rosen JM, Robinson GW, Hennighausen L** 2001 Signal transducer and activator of transcription (Stat) 5 controls the proliferation and differentiation of mammary alveolar epithelium. *J Cell Biol* 155:531-42
36. **Woodward TL, Mienaltowski AS, Modi RR, Bennett JM, Haslam SZ** 2001 Fibronectin and the  $\alpha(5)\beta(1)$  integrin are under developmental and ovarian steroid regulation in the normal mouse mammary gland. *Endocrinology* 142:3214-22
37. **Rosario M, Birchmeier W** 2003 How to make tubes: signaling by the Met receptor tyrosine kinase. *Trends Cell Biol* 13:328-35
38. **Hartmann G, Prospero T, Brinkmann V, Ozcelik C, Winter G, Hepple J, Batley S, Bladt F, Sachs M, Birchmeier C, Birchmeier W, Gherardi E** 1998 Engineered mutants of HGF/SF with reduced binding to heparan sulphate proteoglycans, decreased clearance and enhanced activity in vivo. *Curr Biol* 8:125-34
39. **Niranjan B, Buluwela L, Yant J, Perusinghe N, Atherton A, Phippard D, Dale T, Gusterson B, Kamalati T** 1995 HGF/SF: a potent cytokine for mammary growth, morphogenesis and development. *Development* 121:2897-908
40. **Yang Y, Spitzer E, Meyer D, Sachs M, Niemann C, Hartmann G, Weidner KM, Birchmeier C, Birchmeier W** 1995 Sequential requirement of hepatocyte growth factor and neuregulin in the morphogenesis and differentiation of the mammary gland. *J Cell Biol* 131:215-26
41. **Furge KA, Zhang YW, Vande Woude GF** 2000 Met receptor tyrosine kinase: enhanced signaling through adapter proteins. *Oncogene* 19:5582-9
42. **Soriano JV, Pepper MS, Nakamura T, Orci L, Montesano R** 1995 Hepatocyte growth factor stimulates extensive development of branching duct-like structures by cloned mammary gland epithelial cells. *J Cell Sci* 108 ( Pt 2):413-30
43. **Haslam SZ, Woodward TL** 2003 Host microenvironment in breast cancer development: epithelial-cell-stromal-cell interactions and steroid hormone action in normal and cancerous mammary gland. *Breast Cancer Res* 5:208-15
44. **Gallego MI, Bieri B, Hennighausen L** 2003 Targeted expression of HGF/SF in mouse mammary epithelium leads to metastatic adenosquamous carcinomas

through the activation of multiple signal transduction pathways. *Oncogene* 22:8498-508

45. **Pollack AL, Runyan RB, Mostov KE** 1998 Morphogenetic mechanisms of epithelial tubulogenesis: MDCK cell polarity is transiently rearranged without loss of cell-cell contact during scatter factor/hepatocyte growth factor-induced tubulogenesis. *Dev Biol* 204:64-79
46. **O'Brien LE, Tang K, Kats ES, Schutz-Geschwender A, Lipschutz JH, Mostov KE** 2004 ERK and MMPs sequentially regulate distinct stages of epithelial tubule development. *Dev Cell* 7:21-32
47. **Williams MJ, Clark P** 2003 Microscopic analysis of the cellular events during scatter factor/hepatocyte growth factor-induced epithelial tubulogenesis. *J Anat* 203:483-503
48. **Takeuchi K, Shibamoto S, Nagamine K, Shigemori I, Omura S, Kitamura N, Ito F** 2001 Signaling pathways leading to transcription and translation cooperatively regulate the transient increase in expression of c-Fos protein. *J Biol Chem* 276:26077-83
49. **Courtneidge SA** 2002 Role of Src in signal transduction pathways. The Jubilee Lecture. *Biochem Soc Trans* 30:11-7
50. **Monga SP, Mars WM, Pediaditakis P, Bell A, Mule K, Bowen WC, Wang X, Zarnegar R, Michalopoulos GK** 2002 Hepatocyte growth factor induces Wnt-independent nuclear translocation of beta-catenin after Met-beta-catenin dissociation in hepatocytes. *Cancer Res* 62:2064-71
51. **Sergeant N, Lyon M, Rudland PS, Fernig DG, Delehedde M** 2000 Stimulation of DNA synthesis and cell proliferation of human mammary myoepithelial-like cells by hepatocyte growth factor/scatter factor depends on heparan sulfate proteoglycans and sustained phosphorylation of mitogen-activated protein kinases p42/44. *J Biol Chem* 275:17094-9
52. **Xiao GH, Jeffers M, Bellacosa A, Mitsuuchi Y, Vande Woude GF, Testa JR** 2001 Anti-apoptotic signaling by hepatocyte growth factor/Met via the phosphatidylinositol 3-kinase/Akt and mitogen-activated protein kinase pathways. *Proc Natl Acad Sci U S A* 98:247-52
53. **Koch A, Mancini A, El Bounkari O, Tamura T** 2005 The SH2-domain-containing inositol 5-phosphatase (SHIP)-2 binds to c-Met directly via tyrosine residue 1356 and involves hepatocyte growth factor (HGF)-induced lamellipodium formation, cell scattering and cell spreading. *Oncogene* 24:3436-47

54. **Huguet EL, Smith K, Bicknell R, Harris AL** 1995 Regulation of Wnt5a mRNA expression in human mammary epithelial cells by cell shape, confluence, and hepatocyte growth factor. *J Biol Chem* 270:12851-6
55. **Beviglia L, Kramer RH** 1999 HGF induces FAK activation and integrin-mediated adhesion in MTLn3 breast carcinoma cells. *Int J Cancer* 83:640-9
56. **Rahimi N, Tremblay E, Elliott B** 1996 Phosphatidylinositol 3-kinase activity is required for hepatocyte growth factor-induced mitogenic signals in epithelial cells. *J Biol Chem* 271:24850-5
57. **Wiseman BS, Sternlicht MD, Lund LR, Alexander CM, Mott J, Bissell MJ, Soloway P, Itohara S, Werb Z** 2003 Site-specific inductive and inhibitory activities of MMP-2 and MMP-3 orchestrate mammary gland branching morphogenesis. *J Cell Biol* 162:1123-33
58. **Sympson CJ, Talhouk RS, Alexander CM, Chin JR, Clift SM, Bissell MJ, Werb Z** 1994 Targeted expression of stromelysin-1 in mammary gland provides evidence for a role of proteinases in branching morphogenesis and the requirement for an intact basement membrane for tissue-specific gene expression. *J Cell Biol* 125:681-93
59. **Sternlicht MD, Bissell MJ, Werb Z** 2000 The matrix metalloproteinase stromelysin-1 acts as a natural mammary tumor promoter. *Oncogene* 19:1102-13
60. **Simian M, Hirai Y, Navre M, Werb Z, Lochter A, Bissell MJ** 2001 The interplay of matrix metalloproteinases, morphogens and growth factors is necessary for branching of mammary epithelial cells. *Development* 128:3117-31
61. **Lee PP, Hwang JJ, Mead L, Ip MM** 2001 Functional role of matrix metalloproteinases (MMPs) in mammary epithelial cell development. *J Cell Physiol* 188:75-88
62. **Haslam SZ, Lively ML** 1985 Estrogen responsiveness of normal mouse mammary cells in primary cell culture: association of mammary fibroblasts with estrogenic regulation of progesterone receptors. *Endocrinology* 116:1835-44
63. **Mote PA, Leary JA, Clarke CL** 1998 Immunohistochemical detection of progesterone receptors in archival breast cancer. *Biotech Histochem* 73:117-27.
64. **Sunil N, Bennett JM, Haslam SZ** 2002 Hepatocyte growth factor is required for progestin-induced epithelial cell proliferation and alveolar-like morphogenesis in serum-free culture of normal mammary epithelial cells. *Endocrinology* 143:2953-60



65. **Haslam SZ, Counterman LJ, St. John AR** 1993 Hormonal basis for acquisition of estrogen-dependent progesterone receptors in the normal mouse mammary gland. *Steroid Biochem. (Life Sci. Adv.)* 12:27-34
66. **Okano J, Shiota G, Matsumoto K, Yasui S, Kurimasa A, Hisatome I, Steinberg P, Murawaki Y** 2003 Hepatocyte growth factor exerts a proliferative effect on oval cells through the PI3K/AKT signaling pathway. *Biochem Biophys Res Commun* 309:298-304
67. **Diehl JA, Cheng M, Roussel MF, Sherr CJ** 1998 Glycogen synthase kinase-3 $\beta$  regulates cyclin D1 proteolysis and subcellular localization. *Genes Dev* 12:3499-511
68. **Abounader R, Reznik T, Colantuoni C, Martinez-Murillo F, Rosen EM, Laterra J** 2004 Regulation of c-Met-dependent gene expression by PTEN. *Oncogene* 23:9173-82
69. **Said TK, Conneely OM, Medina D, O'Malley BW, Lydon JP** 1997 Progesterone, in addition to estrogen, induces cyclin D1 expression in the murine mammary epithelial cell, in vivo. *Endocrinology* 138:3933-9.
70. **Zhang HZ, Bennett JM, Smith KT, Sunil N, Haslam SZ** 2002 Estrogen mediates mammary epithelial cell proliferation in serum-free culture indirectly via mammary stroma-derived hepatocyte growth factor. *Endocrinology* 143:3427-34
71. **Shyamala G, Yang X, Cardiff RD, Dale E** 2000 Impact of progesterone receptor on cell-fate decisions during mammary gland development. *Proc Natl Acad Sci U S A* 97:3044-9.
72. **Lange CA, Shen T, Horwitz KB** 2000 Phosphorylation of human progesterone receptors at serine-294 by mitogen-activated protein kinase signals their degradation by the 26S proteasome. *Proc Natl Acad Sci U S A* 97:1032-7.
73. **Royal I, Lamarche-Vane N, Lamorte L, Kaibuchi K, Park M** 2000 Activation of cdc42, rac, PAK, and rho-kinase in response to hepatocyte growth factor differentially regulates epithelial cell colony spreading and dissociation. *Mol Biol Cell* 11:1709-25
74. **Yu W, O'Brien LE, Wang F, Bourne H, Mostov KE, Zegers MM** 2003 Hepatocyte growth factor switches orientation of polarity and mode of movement during morphogenesis of multicellular epithelial structures. *Mol Biol Cell* 14:748-63
75. **Hellman NE, Greco AJ, Rogers KK, Kanchagar C, Balkovetz DF, Lipschutz JH** 2005 Activated Extracellular Signal Regulated Kinases (ERKs) are Necessary

and Sufficient to Initiate Tubulogenesis in Renal Tubular MDCK Strain I Cell Cysts. *Am J Physiol Renal Physiol*

76. **Choi J, Park SY, Joo CK** 2004 Hepatocyte growth factor induces proliferation of lens epithelial cells through activation of ERK1/2 and JNK/SAPK. *Invest Ophthalmol Vis Sci* 45:2696-704
77. **Lange CA** 2004 Making sense of cross-talk between steroid hormone receptors and intracellular signaling pathways: who will have the last word? *Mol Endocrinol* 18:269-78
78. **Brennan KR, Brown AM** 2004 Wnt proteins in mammary development and cancer. *J Mammary Gland Biol Neoplasia* 9:119-31
79. **Rahimi N, Hung W, Tremblay E, Saulnier R, Elliott B** 1998 c-Src kinase activity is required for hepatocyte growth factor-induced motility and anchorage-independent growth of mammary carcinoma cells. *J Biol Chem* 273:33714-21